http://dx.doi.org/10.5935/0103-5053.20150148

J. Braz. Chem. Soc., Vol. 26, No. 12, 2496-2506, 2015.
Printed in Brazil - ©2015 Sociedade Brasileira de Química
0103 - 5053 $6.00+0.00

Article

Synthesis and Photophysical Characterization of Novel ESIPT Triazinyl-Benzazole Derivatives

Fábio S. Grasel,[a,b] Fabiano Barreto,[c] Louise Jank[a,c] and Valter Stefani*[,a]*

[a]*Instituto de Química, Universidade Federal do Rio Grande do Sul, CP 15003, 91501-970 Porto Alegre-RS, Brazil*

[b]*Programa de Pós-graduação em Engenharia e Tecnologia de Materiais, Pontifícia Universidade Católica do Rio Grande do Sul, CP 1429, 90619-900 Porto Alegre-RS, Brazil*

[c]*Laboratório Nacional Agropecuário - LANAGRO/RS, Ministério da Agricultura, Pecuária e Abastecimento, 91780-580 Porto Alegre-RS, Brazil*

In this work, the synthesis, characterization and photophysical study of new derivatives of triazinyl-benzazoles with fluorescence by excited-state intramolecular proton transfer (ESIPT) are presented. It regards the synthesis of cyanuric chloride with different 2-(2'-hydroxyphenyl) benzazoles, two quite attractive groups from the synthetic and technological point of view. These new compounds have several potential applications such as biological markers and new photoluminescent materials. The derivatives were characterized by ^{1}H and ^{13}C nuclear magnetic resonance (NMR), Fourier transform infrared spectroscopy (FTIR), high-resolution mass spectrometry (HRMS), UV-Vis absorption and fluorescence emission. The dyes are fluorescent by an excited-state ESIPT in the blue-orange region, with a large Stokes' shift.

Keywords: benzazole, cyanuric chloride, ESIPT, reactive dye, large Stokes' shift, fluorescence

Introduction

2,4,6-Trichloro-1,3,5-triazine, also known as cyanuric chloride (TCT) has been widely studied due to its synthetic versatility because it is a very reactive molecule that presents an easily controlled reaction behavior with nucleophiles (Scheme 1).[1-7]

Because of this behavior, TCT presents several applications, such as: producing new polymeric materials,[8-12] as a chiral stationary phase in high-performance liquid chromatography (HPLC),[13] obtaining fluorescent oligomers,[12,14,15] as a precursor of herbicides for the agrochemical industry,[16-19] anti-bactericides,[20-22] and antimicrobials.[23,24] Another important application for TCT and its derivatives is in the dye industry. These dyes have a reactive triazinic group that is able to form a covalent bond with the fibers of several fabrics, mainly cotton.[25-28] The hydroxyl, thiol or amino groups present in cellulose (cotton),[25-29] polyamides, or proteins,[25,30] respectively, can substitute the chlorine atoms of TCT. TCT has also been employed to obtain optical whiteners.[31]

Polymers, natural fibers and paper tend to darken or yellow after some time due to the weak absorption of light in the zone of 400 nm by certain groups: peptides in wool or

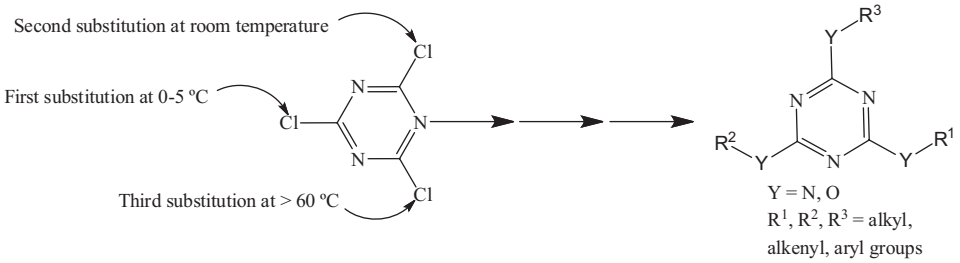

Scheme 1. Differential reactivity of TCT towards nucleophiles.[2-4]

*e-mail: fsgrasel@gmail.com, vstefani@iq.ufrgs.br

silk, flavonoids in cellulose, and products of decomposition in polymers.[31,32] One of the solutions used to reduce or even eliminate this effect is to add optical whiteners. They increase the whiteness of the material by a process of light absorption in the ultraviolet region (330-380 nm) and posterior emission of light in the visible region (400-450 nm). These optical whiteners are obtained from the reaction of the TCT with chromophore groups and are used in papers, woven fabric, detergents, soaps and polymers.[12,14,25,26,30]

Benzazole dyes are a class of chromophores extensively studied because of their very interesting photophysical properties.[33-39] This class of molecules presents a large Stokes' shift due to the intramolecular proton transfer (ESIPT) mechanism (Scheme 2).[33-39]

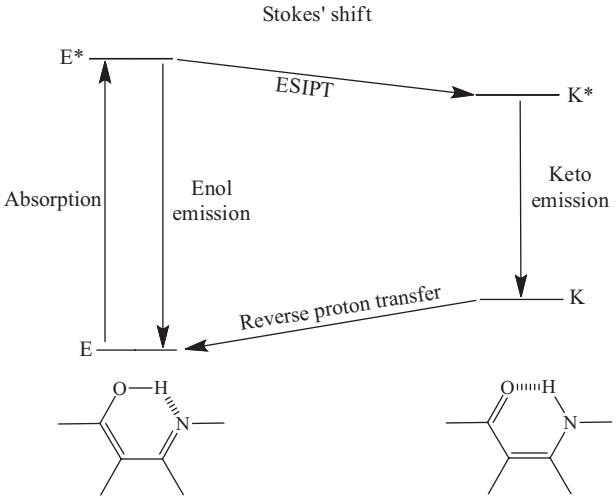

Scheme 2. Photophysical pathways from ESIPT-exhibiting dyes: enol (or normal) emission (left) and ESIPT (or tautomer) emission (right).

The mechanism of ESIPT provides physical and chemical properties to this class of molecules that make them highly attractive from the synthetic, technological and biological point of view.[34-44] Several applications of this type of molecule are described in the literature, such as stabilization of polymers against UV radiation,[45] fluorescent sensors,[43] photoactive materials for organic light emitting diodes,[46,47] molecular switches controlled by light,[48] and optical materials.[49] This paper presents the synthesis, characterization, and photophysical study of new fluorescent triazinyl-benzazole derivatives which present excited-state ESIPT.

Experimental

Materials and methods

The 2,4,6-trichloro-1,3,5-triazine was supplied by ACROS Organics. Spectroscopic grade solvents (Merck) were used for fluorescence and UV-Vis measurements. All the chemicals were analytical grade and were used as received. The reactions were monitored by thin layer chromatography (TLC) on ALUGRAM® SIL Macherey-Nagel silicagel plates. Dichloromethane was used as eluent and the plates were visualized under UV light (254-365 nm). The dyes were purified by column chromatography using silica gel 60 (70-230 mesh ASTM) and dichloromethane. Infrared (IR) spectra were recorded on a Shimadzu FTIR8300 in nujol. The ^{1}H and ^{13}C nuclear magnetic resonance (NMR) spectra were performed at room temperature on an INOVA YH300 using tetramethylsilane (TMS) as the internal standard and DMSO-d_6 as the solvent. The chemical shifts (δ) are reported in parts *per* million (ppm) relative to TMS. The coupling constants J are reported in Hz. The following abbreviations are used for the multiplicities: s (singlet), d (doublet), dd (double of doublets), t (triplet), q (quartet), m (multiplet) and br s (broad singlet). UV-Vis absorption spectra were performed on a Shimadzu UV-1601PC spectrophotometer. Steady state fluorescence spectra were measured with a Hitachi spectrofluorometer model F-4500. Spectrum correction was performed to enable measuring a true spectrum by eliminating instrumental responses such as wavelength characteristics of the monochromator or detector using rhodamine B as a standard (quantum counter). For the photophysical measurements in the solid state, the samples were measured using a solid sample holder. In this device, the light beam irradiated the sample at an angle of approximately 30° and the emitted light from the sample was detected at an angle of approximately 60°. All experiments were performed at room temperature in a concentration of 10^{-6} mol L^{-1}. The high-resolution mass spectrometry (HRMS) spectra analyses were performed on a Bruker Reflex III spectrometer or an Agilent 1100 series liquid chromatograph coupled to an API 5000 triple quadrupole mass spectrometer equipped with an electrospray ionization interface (ESI). Melting points (mp) were measured with a Gehaka PF 1000 apparatus and are uncorrected.

Synthesis of triazinyl-benzazole derivatives

The dyes **2a**-**d** were prepared using a methodology previously described in the literature.[50] The synthesis of the monosubstituted triazinyl-derivatives (**3a**-**d**) was also performed as described in recent literature.[26] The reaction consisted of the addition of benzazole-precursors (**2a**-**d**) in a TCT solution in acetone (1:1) containing sodium carbonate (Na_2CO_3). The reactions were stirred for 1 hour at 0-5 °C. The synthesis of the disubstituted triazinyl-derivatives (**4a**-**d**) comprised adding the benzazole-precursors (**2a**-**d**) in a TCT solution in acetone (2:1), also at 0-5 °C, containing

Na_2CO_3. The reactions were stirred for 12 hours at room temperature. The synthesis of the trisubstituted triazinyl-derivatives (**5a**-**d**) comprised adding the benzazole-precursors (**2a**-**d**) in a TCT solution in acetone (3:1), also at 0-5 °C, containing Na_2CO_3. The reactions were refluxed for 24 hours. The Na_2CO_3 (10%, m/v) was added stoichiometrically in relation to the hydrochloric acid (HCl) formed in the reaction. Distilled water was added to complete precipitation of the product in the end. The products were filtered, washed with distilled water, dried and purified on silica gel columns with dichloromethane as eluent. The final yields were from 70 to 95%. Scheme 3 presents the synthesis of the triazinyl-benzazole derivatives: mono (**3a**-**d**), di (**4a**-**d**) and trisubstituted (**5a**-**d**).

2-[4'-(*N*-4,6-Dichloro-1,3,5-triazin-2-yl)-2'-hydroxyphenyl] benzoxazole (**3a**)

Yield 70%; white solid; mp: decomposed before melting; IR (nujol) ν_{max} / cm^{-1}: 3433 ν(OH), 3298 ν(NH), 1612 ν(C=N), 1533, 1492 and 1452 ν_{arom}(C=C), 1232 ν(Ar-O), 1184 ν(C–N); ^{1}H NMR (300 MHz, DMSO-d_6), δ 11.21 (s, 1H, OH), 10.96 (s, 1H, NH), 7.98 (d, 1H, *J* 8.7 Hz, phenolic-H), 7.78-7.88 (m, 2H, Ar-H), 7.66 (d, 1H, *J* 2.1 Hz, phenolic-H), 7.42-7.48 (m, 2H, Ar-H), 7.21 (dd, 1H, *J* 8.7, 2.1 Hz, phenolic-H); ^{13}C NMR (75.4 MHz, DMSO-d_6) δ 162.2 (C_2), 158.4 ($C_{4'a}$), 153.9 ($C_{4'b}$ and $C_{4'c}$), 152.8 ($C_{2'}$), 148.8 (C_8), 142.2 ($C_{4'}$), 138.8 (C_9), 128.2 (C_5), 125.8 (C_6 or $C_{6'}$), 125.3 ($C_{6'}$ or C_6), 119.0 (C_4), 112.0 ($C_{3'}$ or C_7), 111.0 (C_7 or $C_{3'}$), 107.8 ($C_{5'}$), 105.8 ($C_{1'}$); HRMS (MALDI) *m/z*, calcd. for $C_{16}H_9Cl_2N_5O_2$ [M + H]$^+$: 373.0113; found: 373.0125.

2-[5'-(*N*-4,6-Dichloro-1,3,5-triazin-2-yl)-2'-hydroxyphenyl] benzoxazole (**3b**)

Yield 85%; white solid; mp: decomposed before melting; IR (nujol) ν_{max} / cm^{-1}: 3453 ν(OH), 3296 ν(NH), 1581 ν(C=N), 1502 and 1456 ν_{arom}(C=C), 1297 ν(Ar-O), 1241 ν(C–N); ^{1}H NMR (300 MHz, DMSO-d_6) δ 11.18 (s, 1H, OH), 10.76 (s, 1H, NH), 8.23 (d, 1H, *J* 2.7 Hz, phenolic-H), 7.89-7.84 (m, 2H, Ar-H), 7.66 (dd, 1H, *J* 8.7, 2.7 Hz, phenolic-H), 7.50-7.46 (m, 2H, Ar-H), 7.15 (d, 1H, *J* 8.7 Hz, phenolic-H); ^{13}C NMR (75.4 MHz, DMSO-d_6) δ 169.8 (C_2), 163.8 ($C_{4'a}$), 162.0 ($C_{4'b}$ and $C_{4'c}$), 154.8 ($C_{2'}$), 149.0 (C_8), 139.8 (C_9), 128.8 ($C_{4'}$), 126.6 (C_5 or C_6), 125.2 (C_5 or C_6), 120.8 (C_4), 119.4 ($C_{6'}$ or $C_{3'}$), 118.0 ($C_{3'}$ or $C_{6'}$), 111.1 (C_7), 110.2 ($C_{1'}$); HRMS (MALDI) *m/z*, calcd. for $C_{16}H_9Cl_2N_5O_2$ [M + H]$^+$: 373.0113; found: 373.0127.

2-[4'-(*N*-4,6-Dichloro-1,3,5-triazin-2-yl)-2'-hydroxyphenyl] benzothiazole (**3c**)

Yield 80%; light green solid; mp: decomposed before melting; IR (nujol) ν_{max} / cm^{-1}: 3451 ν(OH), 3328 ν(NH), 1610 ν(C=N), 1548 and 1461 ν_{arom}(C=C), 1235 ν(Ar-O), 1180 ν(C–N); ^{1}H NMR (300 MHz, DMSO-d_6) δ 11.19 (s, 1H, OH), 10.85 (s, 1H, NH), 8.24 (d, 1H, *J* 2.7 Hz, phenolic-H), 7.89-7.85 (m, 2H, Ar-H), 7.72 (dd, 1H, *J* 9.0 Hz, phenolic-H), 7.51-7.47 (m, 2H, Ar-H), 7.19 (d, 1H, *J* 9.0 Hz, phenolic-H); ^{13}C NMR (75.4 MHz, DMSO-d_6) δ 169.9 (C_2), 164.0 ($C_{4'a}$), 162.0 ($C_{4'b}$ and $C_{4'c}$), 155.0 ($C_{2'}$), 148.8 (C_9), 139.8 ($C_{4'}$), 129.0 (C_8), 128.1 (C_4), 126.0 (C_5 or C_6), 125.3 (C_5 or C_6), 120.7 ($C_{6'}$), 119.4 (C_7 or $C_{3'}$), 118.0 ($C_{3'}$ or C_7), 111.4 ($C_{5'}$), 110.2 ($C_{1'}$); HRMS (MALDI) *m/z*, calcd. for $C_{16}H_9Cl_2N_5O_2$ [M + H]$^+$: 388.9903; found: 388.9905.

2-[5'-(*N*-4,6-Dichloro-1,3,5-triazin-2-yl)-2'-hydroxyphenyl] benzothiazole (**3d**)

Yield 80%; yellow solid; mp: decomposed before melting; IR (nujol) ν_{max} / cm^{-1}: 3454 ν(OH), 3293 ν(NH), 1595 ν(C=N), 1549, 1502 and 1456 ν_{arom}(C=C),

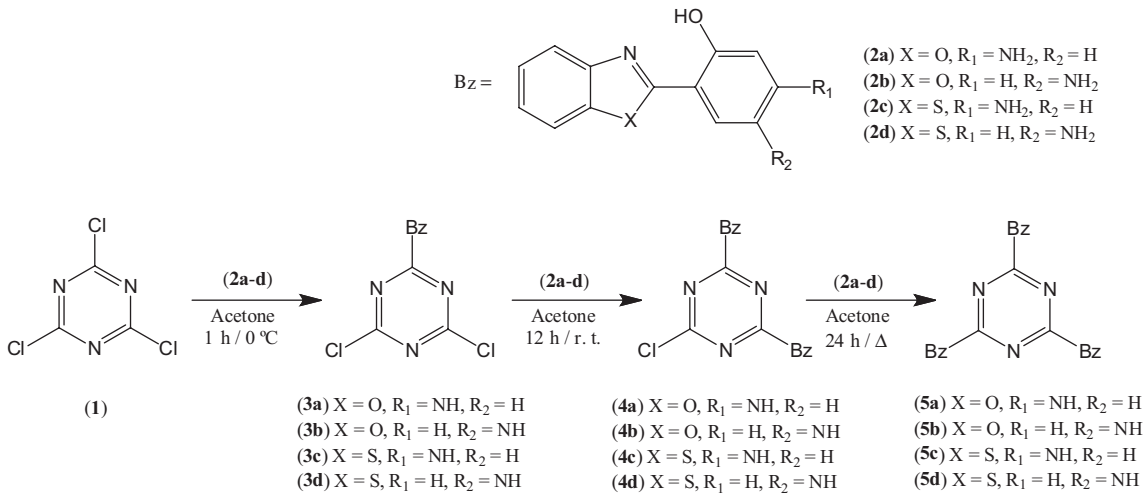

Scheme 3. Synthesis of mono (**3a**-**d**), di (**4a**-**d**) and trisubstituted (**5a**-**d**) triazinyl-benzazole derivatives.

1241 ν(Ar-O), 1194 ν(C–N); ^{1}H NMR (300 MHz, DMSO-d_6) δ 11.09 (s, 1H, OH), 10.90 (s, 1H, NH), 8.41 (d, 1H, *J* 2.7 Hz, phenolic-H), 7.62-7.58 (m, 2H, Ar-H), 7.60 (dd, 1H, *J* 9.0, 2.7 Hz, phenolic-H), 7.57-7.52 (m, 2H, Ar-H), 7.13 (d, 1H, *J* 9.0 Hz, phenolic-H); ^{13}C NMR (75.4 MHz, DMSO-d_6) δ 169.9 (C_2), 168.9 ($C_{5'a}$), 163.9 ($C_{5'b}$ or $C_{5'c}$), 153.8 ($C_{2'}$), 151.3 (C_9), 134.8 ($C_{5'}$), 129.0 (C_8), 127.4 (C_5 or C_6), 126.7 (C_5 or C_6), 124.8 (C_4), 122.2 (C_7 or $C_{4'}$), 122.0 ($C_{4'}$ or C_7), 119.8 ($C_{6'}$), 118.2 ($C_{1'}$), 117.3 ($C_{3'}$); HRMS (MALDI) *m/z*, calcd. for $C_{16}H_9Cl_2N_5O_2$ [M + H]$^+$: 388.9903; found: 388.9897.

2,4-Di[2-(4'-aminyl-2'-hydroxphenyl)benzoxazole]-6-chloro-1,3,5-triazine (**4a**)

Yield 80%; white solid; mp: decomposed before melting; IR (nujol) ν_{max} / cm^{-1}: 3454 ν(OH), 3295 ν(NH), 1619 ν(C=N), 1535, 1498 and 1451 ν_{arom}(C=C), 1236 ν(Ar-O), 1180 ν(C–N); ^{1}H NMR (300 MHz, DMSO-d_6) δ 11.46 (s, 2H, 2OH), 10.94 (s, 2H, 2NH), 8.08 (d, 2H, *J* 8.4 Hz, 2phenolic-H), 7.75 (d, 2H, *J* 1.8 Hz, 2phenolic-H), 7.72-7.60 (m, 4H, 2Ar-H), 7.44-7.37 (m, 4H, 2Ar-H), 7.14 (dd, 2H, *J* 8.4, 1.8 Hz, 2phenolic-H); HRMS (ESI) *m/z*, calcd. for $C_{29}H_{18}ClN_7O_4$ [M + H]$^+$: 564.1187; found: 564.1191; HRMS (ESI) *m/z*, calcd. for $C_{29}H_{18}ClN_7O_4$ [M – H]$^-$: 562.1030; found: 562.1020.

2,4-Di[2-(5'-aminyl-2'-hydroxphenyl)benzoxazole]-6-chloro-1,3,5-triazine (**4b**)

Yield 80%; white solid; mp: decomposed before melting; IR (nujol) ν_{max} / cm^{-1}: 3418 ν(OH), 3330 ν(NH), 1616 ν(C=N), 1568, 1524 and 1498 ν_{arom}(C=C), 1235 ν(Ar-O), 1173 ν(C–N); ^{1}H NMR (300 MHz, DMSO-d_6) δ 10.59 (s, 2H, 2OH), 10.40 (s, 2H, 2NH), 8.62 (s, 2H, 2phenolic-H), 7.54-7.47 (m, 4H, 2Ar-H), 7.36 (d, 2H, *J* 8.1 Hz, 2phenolic-H), 7.16-7.28 (m, 4H, 2Ar-H), 7.04 (d, 2H, *J* 8.1 Hz, 2phenolic-H); HRMS (ESI) *m/z*, calcd. for $C_{29}H_{18}ClN_7O_4$ [M + H]$^+$: 564.1187; found: 564.1207; HRMS (ESI) *m/z*, calcd. for $C_{29}H_{18}ClN_7O_4$ [M – H]$^-$: 562.1030; found: 562.1041.

2,4-Di[2-(4'-aminyl-2'-hydroxphenyl)benzothiazole]-6-chloro-1,3,5-triazine (**4c**)

Yield 75%; light green solid; mp: decomposed before melting; IR (nujol) ν_{max} / cm^{-1}: 3454 ν(OH), 3333 ν(NH), 1609 ν(C=N), 1544 and 1460 ν_{arom}(C=C), 1236 ν(Ar-O), 1180 ν(C–N); ^{1}H NMR (300 MHz, DMSO-d_6) δ 11.05 (s, 2H, 2OH), 10.73 (s, 2H, 2NH), 8.26 (d, 2H, *J* 8.4, 2phenolic-H), 8.19-7.97 (m, 4H, 2Ar-H), 7.72 (d, 2H, *J* 1.8 Hz, 2phenolic-H), 7.57-6.93 (m, 4H, 2Ar-H), 7.09 (dd, 2H, *J* 8.4, 1.8 Hz, 2phenolic-H); HRMS (ESI) *m/z*, calcd. for $C_{29}H_{18}ClN_7O_2S_2$ [M + H]$^+$: 596.0730; found: 596.0755; HRMS (ESI) *m/z*, calcd. for $C_{29}H_{18}ClN_7O_2S_2$ [M – H]$^-$: 594.0573; found: 594.0546.

2,4-Di[2-(5'-aminyl-2'-hydroxphenyl)benzothiazole]-6-chloro-1,3,5-triazine (**4d**)

Yield 70%; beige solid; mp: decomposed before melting; IR (nujol) ν_{max} / cm^{-1}: 3442 ν(OH), 3334 ν(NH), 1605 *ν*(C=N), 1577 and 1502 ν_{arom}(C=C), 1260 ν(Ar-O), 1185 ν(C–N); ^{1}H NMR (300 MHz, DMSO-d_6) δ 8.16 (d, 2H, *J* 1.8 Hz, 2phenolic-H); 8.01-7.85 (m, 4H, 2Ar-H); 7.58 (br, 2H, 2phenolic-H); 7.43-7.26 (m, 4H, 2Ar-H); 6.68 (br, 2H, 2phenolic-H); HRMS (ESI) *m/z*, calcd. for $C_{29}H_{18}ClN_7O_2S_2$ [M + H]$^+$: 596.0730; found: 596.0732; HRMS (ESI) *m/z*, calcd. for $C_{29}H_{18}ClN_7O_2S_2$ [M – H]$^-$: 594.0573; found: 594.0572.

2,4,6-Tri[2-(4'-aminyl-2'-hydroxphenyl)benzoxazole]-1,3,5-triazine (**5a**)

Yield 75%; white solid; mp: decomposed before melting; IR (nujol) ν_{max} / cm^{-1}: 3494 ν(OH), 3379 ν(NH), 1641 ν(C=N), 1467 and 1388 ν_{arom}(C=C), 1246 ν(Ar-O), 1188 ν(C–N); ^{1}H NMR (300 MHz, DMSO-d_6) δ 11.63 (s, 3H, 3OH), 7.68 (m, 6H, 3Ar-H and 3H, 3phenolic-H), 7.34 (m, 6H, 3Ar-H), 6.28 (dd, 3H, *J* 8.8, 2.3 Hz, 3phenolic-H), 6.18 (d, 3H, *J* 2.3, 3phenolic-H), 6.10 (s, 3H, 3NH); HRMS (ESI) *m/z*, calcd. for $C_{16}H_9Cl_2N_5O_2$ [M + H]$^+$: 754.2163; found: 754.2197; HRMS (ESI) *m/z*, calcd. for $C_{16}H_9Cl_2N_5O_2$ [M – H]$^-$: 752.2006; found: 752.2026.

2,4,6-Tri[2-(5'-aminyl-2'-hydroxphenyl)benzoxazole]-1,3,5-triazine (**5b**)

Yield 80%; white solid; mp: decomposed before melting; IR (nujol) ν_{max} / cm^{-1}: 3457 ν(OH), 3291 ν(NH), 1616 ν(C=N), 1568, 1533 and 1498 ν_{arom}(C=C), 1226 ν(Ar-O), 1173 ν(C–N); ^{1}H NMR (300 MHz, DMSO-d_6) δ 11.18 (s, 3H, 3OH), 10.43 (s, 3H, 3NH), 8.62 (d, 3H, *J* 2.1 Hz, 3phenolic-H), 7.55 (dd, 3H, *J* 8.7, 2.1 Hz, 3phenolic-H), 7.48 (m, 6H, 3Ar-H), 7.37-7.23 (m, 6H, 3Ar-H), 7.05 (d, 3H, *J* 8.7 Hz, 3phenolic-H); HRMS (ESI) *m/z*, calcd. for $C_{42}H_{27}N_9O_6$ [M + H]$^+$: 754.2163; found: 754.2174; HRMS (ESI) *m/z*, calcd. for $C_{42}H_{27}N_9O_6$ [M – H]$^-$: 752.2006; found: 752.2028.

2,4,6-Tri[2-(4'-aminyl-2'-hydroxphenyl)benzothiazole]-1,3,5-triazine (**5c**)

Yield 80%; beige solid; mp: decomposed before melting; IR (nujol) ν_{max} / cm^{-1}: 3464 *ν*(OH), 3370 ν(NH), 1619 ν(C=N), 1465 and 1371 ν_{arom}(C=C), 1193 ν(Ar-O), 1141 ν(C–N); ^{1}H NMR (300 MHz, DMSO-d_6) δ 11.19 (s, 3H, 3OH), 8.03-7.86 (m, 6H, 3Ar-H), 7.62 (d, 3H, *J* 8.8 Hz, 3phenolic-H), 7.48-7.30 (m, 6H, 3Ar-H), 6.25-6.22 (dd,

1H, *J* 8.8, 2.3 Hz, 3phenolic-H), 6.15 (d, 3H, *J* 2.3 Hz, 3phenolic-H), 5.95 (s, 3H, 3NH); HRMS (ESI) *m/z*, calcd. for $C_{42}H_{27}N_9O_3S_3$ $[M+H]^+$: 802.1477; found: 802.1527; HRMS (ESI) *m/z*, calcd. for $C_{42}H_{27}N_9O_3S_3$ $[M - H]^-$: 800.1321; found: 800.1339.

2,4,6-Tri[2-(5'-aminyl-2'-hydroxphenyl)benzothiazole]-1,3,5-triazine (**5d**)

Yield 75%; beige solid; mp: decomposed before melting; IR (nujol) ν_{max} / cm^{-1}: 3431 ν(OH), 3300 *ν*(NH), 1603 ν(C=N), 1461 and 1382 ν_{arom}(C=C), 1241 ν(Ar-O), 1189 ν(C–N); ^{1}H NMR (300 MHz, DMSO-d_6) δ 11.74 (s, 3H, 3OH), 10.06 (s, 3H, 3NH), 8.28 (s, 3H, 3phenolic-H), 8.05-7.98 (m, 6H, 3Ar-H), 7.67 (s, 3H, 3phenolic-H), 7.54-7.40 (m, 6H, 3Ar-H), 6.93 (d, 3H, *J* 8.1 Hz, 3phenolic-H); HRMS (ESI) *m/z*, calcd. for $C_{42}H_{27}N_9O_3S_3$ $[M+H]^+$: 802.1477; found: 802.1510; HRMS (ESI) *m/z*, calcd. for $C_{42}H_{27}N_9O_3S_3$ $[M - H]^-$: 800.1321; found: 800.1333.

Results and Discussion

Photophysical characterization

Figures 1 to 4 present the normalized UV-Vis absorption spectra and fluorescence emission of the derivatives **3a**-**d** in solution. The spectra in the solid state are also presented for comparison. The relevant spectroscopic data from these dyes are summarized in Table 1.

The derivatives **3a**-**d** presented an absorption maximum (λ) in solution in the range of 337 to 355 nm, while in the solid state the range was from 350 to 398 nm. The location of the absorption showed a slight dependence (2-4 nm) on the solvent. This behavior is usually related to the conformational equilibrium in solution in the ground state.[51-55] The molar absorptivity (ε) according to transitions of type π→π* and fluorescence quantum yields (ϕ) showed results in the range from 1.00 to 5.06 10^4 L mol^{-1} cm^{-1} and 0.003 to 0.061, respectively (Table 1).

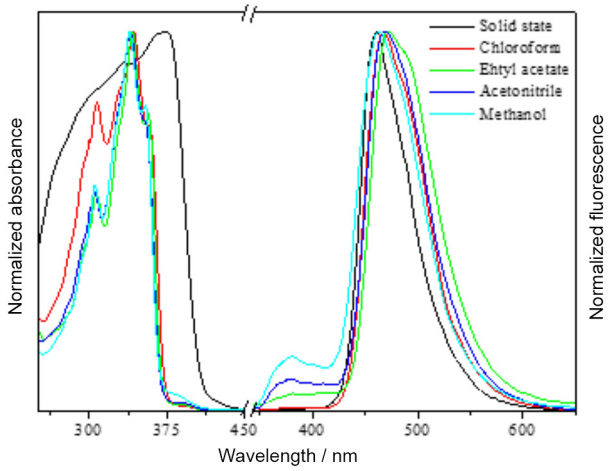

Figure 1. Normalized UV-Vis absorbance and fluorescence emission espectra of **3a**.

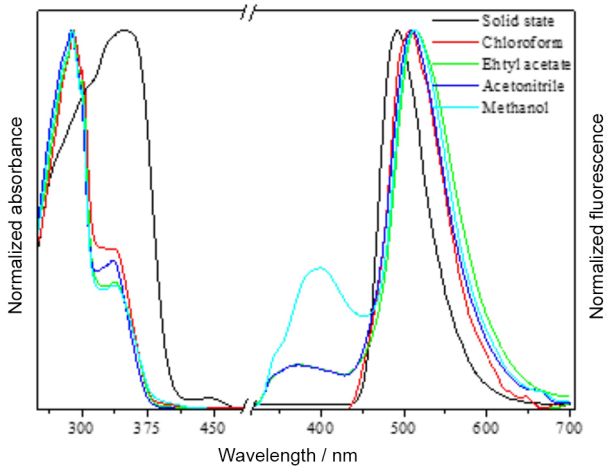

Figure 2. Normalized UV-Vis absorbance and fluorescence emission espectra of **3b**.

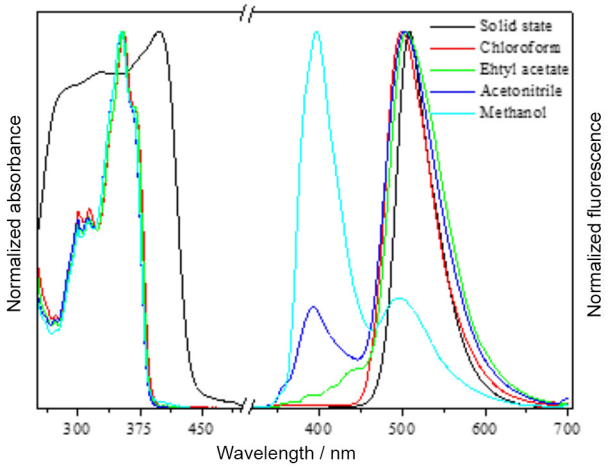

Figure 3. Normalized UV-Vis absorbance and fluorescence emission espectra of **3c**.

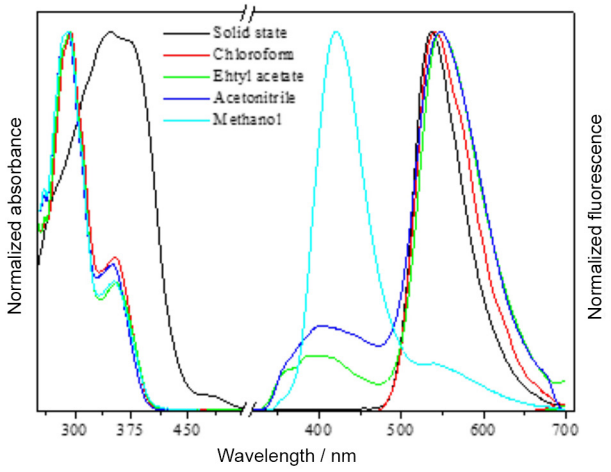

Figure 4. Normalized UV-Vis absorbance and fluorescence emission espectra of **3d**.

Table 1. Data from UV-Vis absorption and fluorescence emission for derivatives **3a-d**

Dye	Solvent	λ^a / nm	$\varepsilon^b \times 10^{-4}$ / (L mol^{-1} cm^{-1})	λ_{enol} / nm	λ_{keto} / nm	$\Delta\lambda_{STenol}$ / nm	$\Delta\lambda_{STketo}$ / nm	ϕ^c
3a	solid state	373	–	–	459	–	–	–
	chloroform	357	4.02	–	467	–	110	0.061
	ethyl acetate	357	3.29	382	470	25	113	0.021
	acetonitrile	353	3.11	380	468	27	115	0.010
	methanol	353	3.49	379	463	26	110	0.016
3b	solid state	350	–	–	492	–	–	–
	chloroform	337	1.22	–	507	–	170	0.009
	ethyl acetate	339	1.02	375	512	36	173	0.010
	acetonitrile	337	1.09	373	508	36	171	0.005
	methanol	339	1.00	396	512	57	173	0.006
3c	solid state	398	–	–	509	–	–	–
	chloroform	354	4.69	–	500	–	146	0.043
	ethyl acetate	352	4.94	440	505	88	153	0.009
	acetonitrile	352	4.80	393	503	41	151	0.004
	methanol	352	5.06	397	498	45	146	0.011
3d	solid state	373	–	–	536	–	–	–
	chloroform	354	1.69	–	540	–	186	0.008
	ethyl acetate	355	1.52	393	549	38	194	0.005
	acetonitrile	351	1.54	402	547	51	196	0.003
	methanol	352	1.44	420	543	68	191	0.006

[a]Absorption maximum; [b]molar absorptivity; [c]fluorescence quantum yields; λ_{enol}: emission of the enol tautomer; λ_{keto}: emission of the keto tautomer; $\Delta\lambda_{STenol}$: Stokes' shift for the emission of enol tautomer; $\Delta\lambda_{STketo}$: Stokes' shift for the emission of keto tautomer.

The wavelength of maximum emission in solution for molecules **3a-d** was in the range of 373 to 440 nm for the enol tautomer and 463 to 549 nm for the keto tautomer. The first Stokes' shift in solution was between 25 and 88 nm (emission of the enol tautomer) and the second one was between 110 and 196 nm (emission of the keto tautomer). Depending on the polarity of the solvent, dual fluorescence emission was observed for all monosubstituted-triazine derivatives (**3a-d**). This behavior is related to the conformational equilibrium in solution in the ground state. The benzothiazole-derivatives (**3c-d**) were more sensitive to the effect of the solvent. The ESIPT mechanism was hardly observed in methanol, with most of the emission being due to the enol tautomer (Scheme 1).

Figures 5 to 8 present normalized UV-Vis absorption spectra and fluorescence emissions of derivatives **4a-d** in solution. The spectra in the solid state are also presented for comparison. The relevant spectroscopic data from these dyes are summarized in Table 2.

The derivatives **4a-d** presented an absorption maximum (λ) in solution in the range of 312 to 361 nm, while in the solid state the range was from 378 to 396 nm. The location of the absorption showed a slight dependence (4-10 nm) on the solvent. This behavior is usually related to the conformational equilibrium in solution in the ground state.[52-56] The molar absorptivity (ε), according to transitions of the type $\pi\rightarrow\pi^*$ and fluorescence quantum yields (ϕ) showed results from 0.55 to 2.51 10^4 L mol^{-1} cm^{-1} and 0.006 to 0.226, respectively (Table 2).

The wavelength of maximum emission in solution for molecules **4a-d** was in the range of 373 to 425 nm for the enol tautomer and 461 to 571 nm for the keto tautomer. The first Stokes' shift was between 23 and 73 nm (emission of the enol tautomer) and the second one was between 110 and 210 nm (emission of the keto tautomer). Dual fluorescence emission was observed for disubstituted-triazine derivatives **4a**, **4c** and **4d** depending on the polarity of the solvent. The derivative **4b** did not show any influence of the solvent on the fluorescence emission. In the analysis of the monosubstituted-triazine derivatives (**3a-d**), the benzothiazole-derivatives were more sensitive to the solvent effect. This effect was not observed for the disubstituted-derivatives (**4a-d**). For the disubstituted group (**4a-d**), the 4'-derivative (**4a** and **4c**) showed greater sensitivity to the solvent than the 5'-derivative (**4b** and **4d**).

It is known that having the amino group located in the *meta*-position relative to the phenolic hydroxyl group

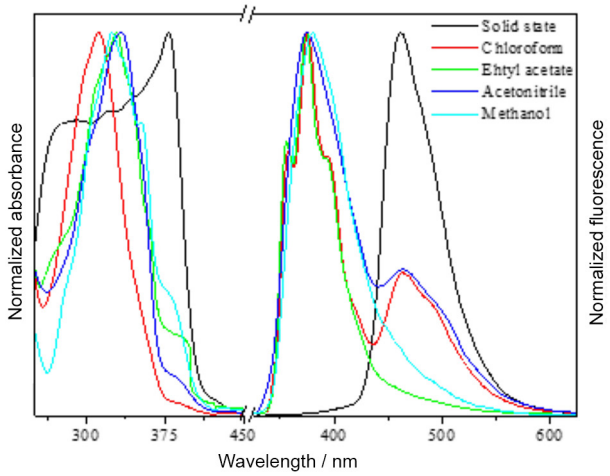

Figure 5. Normalized UV-Vis absorbance and fluorescence emission espectra of **4a**.

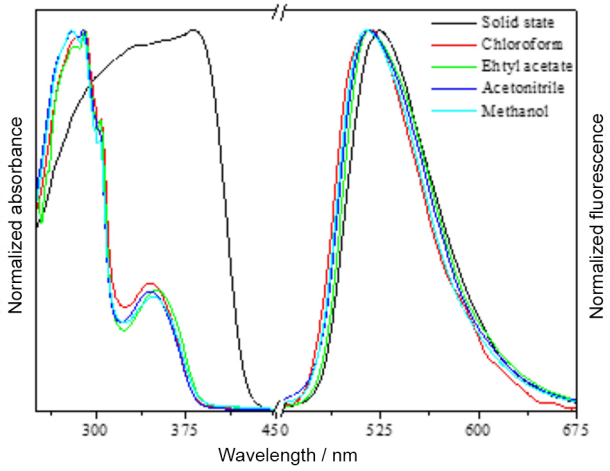

Figure 6. Normalized UV-Vis absorbance and fluorescence emission espectra of **4b**.

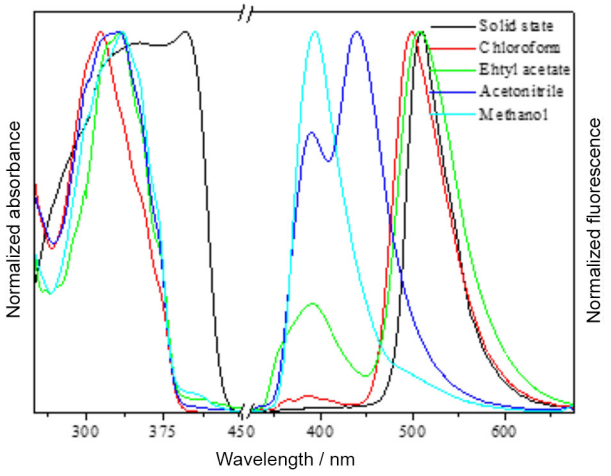

Figure 7. Normalized UV-Vis absorbance and fluorescence emission espectra of **4c**.

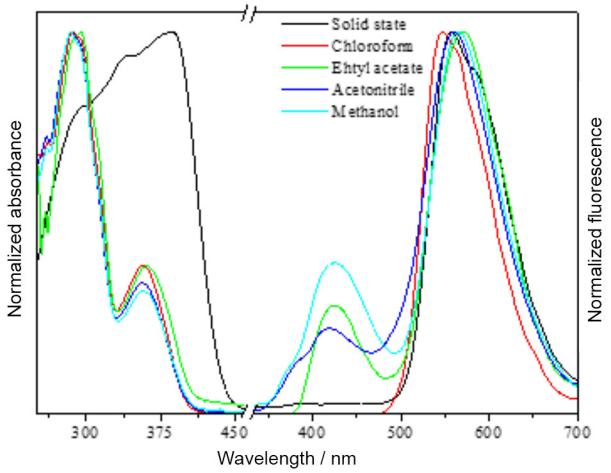

Figure 8. Normalized UV-Vis absorbance and fluorescence emission espectra of **4d**.

(4'-position) weakens the intramolecular hydrogen bond when compared to substituted analogs with the same group in the *para*-position (5'-position). This behavior is observed for disubstituted-derivatives (**4a-d**).[56] However, this behavior was not observed in the monosubstituted-derivatives (**3a-d**) because TCT (**1**), which possesses two chlorine atoms (electron-withdrawing group by inductive effect), is bonded in this amino group. The electron density of the amino group is shifted more to the triazinic ring than to the phenolic ring due to the electron deficiency of the cyanuric chloride.

Figures 9 to 12 present the normalized UV-Vis absorption spectra and fluorescence emission of derivatives **5a-d** in solution. The spectra in the solid state are also presented for comparison. The relevant spectroscopic data from these dyes are summarized in Table 3.

The derivatives **5a-d** presented an absorption maximum (λ) in solution in the range of 334 to 361 nm, while in the solid state the range was from 374 to 409 nm. The location of the absorption showed a slight dependence (4-11 nm) on the solvent. This behavior is usually related to the conformational equilibrium in solution in the ground state.[51-55] The molar absorptivity (ε), according to transitions of the type $\pi \rightarrow \pi^*$, and fluorescence quantum yields (ϕ) showed results from 1.84 to 13.40 10^4 L mol^{-1} cm^{-1} and 0.003 to 0.048, respectively (Table 3).

The trisubstituted-derivatives (**5a-d**) showed higher molar absorptivity (ε) than their mono (**3a-d**), and disubstituted (**4a-d**) analogs. The difference in ε was more pronounced in the derivatives substituted in the 4'-position (**5a** and **5c**) than in those substituted in the 5'-position (**5b** and **5d**). The wavelength of maximum emission in solution for molecules **5a-d** was in the range of 372 to 423 nm for the enol tautomer and 460 to 558 nm for the keto tautomer. The first Stokes' shift was between 27 and 65 nm (emission of the enol tautomer) and the second was between 115 and 201 nm (emission of the keto tautomer), both in solutions. The behavior presented by the trisubstituted-derivatives

Table 2. Data from UV-Vis absorption and fluorescence emission for derivatives **4a-d**

Dye	Solvent	λ^a / nm	$\varepsilon^b \times 10^{-4}$ / (L mol^{-1} cm^{-1})	λ_{enol} / nm	λ_{keto} / nm	$\Delta\lambda_{STenol}$ / nm	$\Delta\lambda_{STketo}$ / nm	ϕ^c
4a	solid state	378	–	–	461	–	–	–
	chloroform	312	1.21	375	464	63	152	0.030
	ethyl acetate	329	0.56	373	–	44	–	0.226
	acetonitrile	336	0.80	374	446	38	110	0.025
	methanol	352	0.55	379	–	27	–	0.025
4b	solid state	382	–	–	523	–	–	–
	chloroform	346	2.15	–	517	–	171	0.022
	ethyl acetate	351	1.92	391	518	40	167	0.016
	acetonitrile	347	1.93	384	515	37	168	0.011
	methanol	349	1.60	388	513	39	164	0.009
4c	solid state	396	–	–	510	–	–	–
	chloroform	314	1.92	387	500	73	186	0.036
	ethyl acetate	333	1.44	391	506	58	173	0.036
	acetonitrile	332	2.51	389	444	57	112	0.019
	methanol	335	1.62	394	–	59	–	0.033
4d	solid state	388	–	–	557	–	–	–
	chloroform	358	1.48	–	547	–	189	0.009
	ethyl acetate	361	1.39	425	571	64	210	0.009
	acetonitrile	357	1.40	419	560	62	203	0.006
	methanol	358	1.03	425	564	67	206	0.006

[a]Absorption maximum; [b]molar absorptivity; [c]fluorescence quantum yields; λ_{enol}: emission of the enol tautomer; λ_{keto}: emission of the keto tautomer; $\Delta\lambda_{STenol}$: Stokes' shift for the emission of enol tautomer; $\Delta\lambda_{STketo}$: Stokes' shift for the emission of keto tautomer.

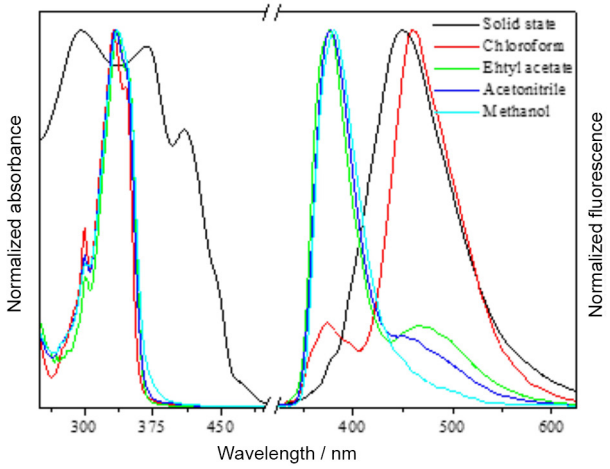

Figure 9. Normalized UV-Vis absorbance and fluorescence emission espectra of **5a**.

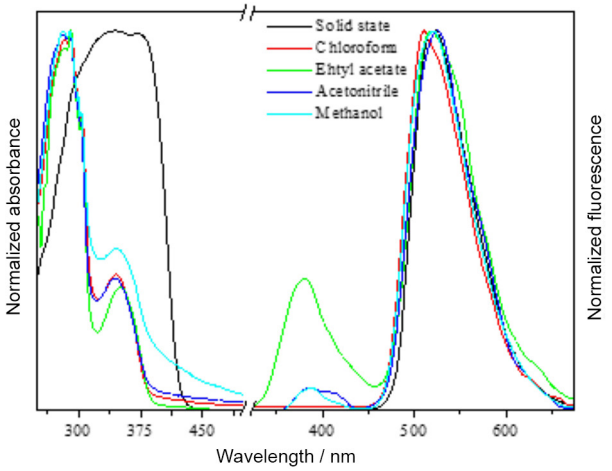

Figure 10. Normalized UV-Vis absorbance and fluorescence emission espectra of **5b**.

(**5a-d**) was the same presented by the disubstituted-derivatives (**4a-d**). The 4'-derivatives (**5a** and **5c**) were more sensitive to the solvent effect than the 5'-derivatives (**5b** and **5d**). The derivatives **3a**, **4a**, **5a**, **3c**, **4c** and **5c**, which have the amino group in the 4'-position, showed a higher fluorescence quantum yield than their respective analogues **3b**, **4b**, **5b**, **3d**, **4d** and **5d**, which have the amino group in the 5'-position. The derivatives with the amino group in the 5'-position (**3b**, **4b**, **5b**, **3d**, **4d** and **5d**) also have a larger Stokes' shift than their analogues with the amino group in the 4'-position (**3a**, **4a**, **5a**, **3c**, **4c** and **5c**). The difference in emissions of the keto tautomers were greater when the molecules were benzothiazole-derivatives rather than benzoxazole ones.

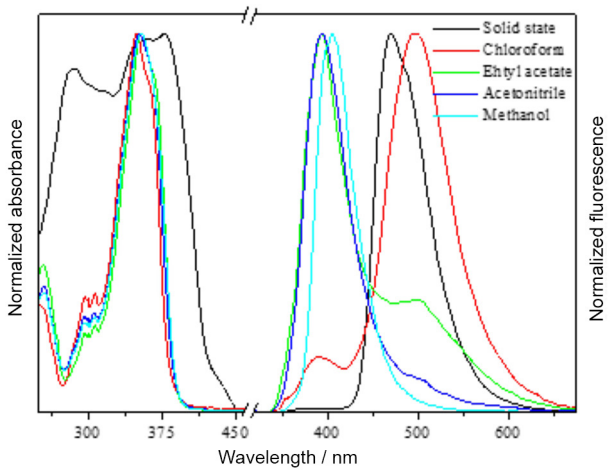

Figure 11. Normalized UV-Vis absorbance and fluorescence emission espectra of **5c**.

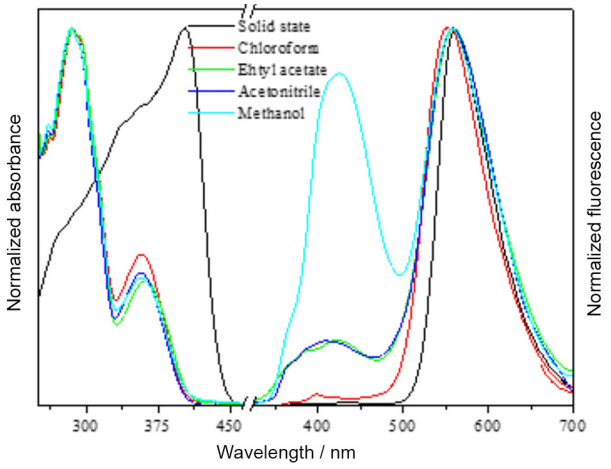

Figure 12. Normalized UV-Vis absorbance and fluorescence emission espectra of **5d**.

Table 3. Data from UV-Vis absorption and fluorescence emission for derivatives **5a**-**d**

Dye	Solvent	λ^a / nm	$\varepsilon^b \times 10^{-4}$ / (L mol^{-1} cm^{-1})	λ_{enol} / nm	λ_{keto} / nm	$\Delta\lambda_{STenol}$ / nm	$\Delta\lambda_{STketo}$ / nm	ϕ^c
5a	solid state	409	–	–	449	–	–	–
	chloroform	345	9.63	372	460	27	115	0.048
	ethyl acetate	335	13.40	377	469	42	134	0.019
	acetonitrile	334	12.47	377	464	43	130	0.016
	methanol	336	12.27	381	–	45	–	0.019
5b	solid state	374	–	–	521	–	–	–
	chloroform	345	2.37	–	511	–	166	0.022
	ethyl acetate	351	1.98	380	517	29	166	0.017
	acetonitrile	345	2.30	387	525	42	180	0.013
	methanol	347	1.84	387	521	40	174	0.017
5c	solid state	378	–	–	470	–	–	–
	chloroform	349	8.52	390	497	41	148	0.010
	ethyl acetate	354	10.02	393	499	39	145	0.007
	acetonitrile	352	9.56	393	–	41	–	0.009
	methanol	354	9.82	405	–	51	–	0.025
5d	solid state	402	–	–	561	–	–	–
	chloroform	357	3.08	400	554	43	197	0.005
	ethyl acetate	361	2.73	417	558	56	197	0.004
	acetonitrile	357	2.73	411	558	54	201	0.003
	methanol	358	2.51	423	557	65	199	0.004

[a]Absorption maximum; [b]molar absorptivity; [c]fluorescence quantum yields; λ_{enol}: emission of the enol tautomer; λ_{keto}: emission of the keto tautomer; $\Delta\lambda_{STenol}$: Stokes' shift for the emission of enol tautomer; $\Delta\lambda_{STketo}$: Stokes' shift for the emission of keto tautomer.

Conclusions

Novel fluorescent triazinyl-benzazoles prepared by the ESIPT mechanism were synthesized, purified and characterized by IR spectroscopy, nuclear magnetic resonance (^{13}C and ^{1}H NMR), HRMS, UV-Vis and steady-state fluorescence spectroscopies (in solution and in the solid state). The properties of derivatives with the amino group in the 5'-position were less affected by the solvent than their analogues with the amino group in the 4'-position. The derivatives with the amino group in the 4'-position presented higher fluorescence quantum yields than their analogues with the amino group in the 5'-position. The trisubstituted-derivatives

showed the highest molar absorptivity (ε) among the derivatives studied. The derivatives with an amino group in the 5'-position exhibited larger Stokes' shift than their analogues with an amino group in the 4'-position of the phenolic ring. This difference was larger in the benzothiazoles than in the benzoxazoles.

Monosubstituted benzothiazole-derivatives showed more intense dual fluorescence than monosubstituted benzoxazole-derivatives. For di and trisubstituted-derivatives, dual fluorescence emission was more intense in the derivatives with the amino group in the 4'-position than their analogues with the amino group in the 5'-position. The derivative 2,4-di[2-(5'-aminyl-2'-hydroxphenyl) benzoxazole]-6-chloro-1,3,5-triazine (**4b**) was the only one where the fluorescence emission of the keto tautomer was not affected by the solvent. The novel ESIPT triazinyl-benzazole derivatives showed very interesting photophysical properties and are promising molecules that could be used to obtain new materials, such as fluorescent sensors and photoluminescent polymers.

Supplementary Information

Supplementary data are available free of charge at http://jbcs.sbq.org.br as PDF file.

Acknowledgments

The authors thank the Programa de Pós-Graduação em Química of the Universidade Federal do Rio Grande do Sul, for the support during the period of this research.

References

1. Thurston, J. T.; Dudley, J. R.; Kaiser, D. W.; Hechenbleikner, I.; Schafer, F. C.; Holm-Hansen, D.; *J. Am. Chem. Soc.* **1951**, *73*, 298.
2. Hoog, P.; Gamez, P.; Driessen, W. L.; Reedijk, J.; *Tetrahedron Lett*. **2002**, *43*, 6783.
3. Blotny, G.; *Tetrahedron* **2006**, *62*, 9507.
4. Gamez, P.; Hoog, P.; Lutz, M.; Spek, A. L.; Reedijk, J.; *Inorg. Chim. Acta* **2003**, *351*, 319.
5. Gajjar, D.; Patel, R.; Patel, H.; Patel, P. M.; *Chem. Sci. Trans.* **2014**, *3*, 897.
6. Lee, J.; Um, S.; Kang, Y.; Baek, D.; *Dyes Pigm.* **2005**, *64*, 25.
7. Hussan, M.; Khan, K. M.; Ali, S. I.; Parveen, R.; Shin, W. S.; *Fibers Polym*. **2009**, *10*, 407.
8. Patel, K. C.; Patel, S. K.; Shal, R. R.; Patel, R. M.; *Iran. J. Polym. Sci. Technol.* **2005**, *4*, 232.
9. Jan, J. Z.; Huang, B. H.; Lin, J. J.; *Polym.* **2003**, *44*, 1003.
10. Son, Y.; Hong, J.; Lim, H.; Kim, T.; *Dyes Pigm.* **2005**, *44,* 231.
11. Wu, H.; Saikia, D.; Chao, H.; Fang, J.; Tsai, L.; Kao, H.; *Electrochim. Acta* **2014**, *138*, 30.
12. Dodangeh, M.; Yousefi, N.; Mohammadian, M.; *Dyes Pigm.* **2015**, *116*, 20.
13. Liebes, L.; Conaway, C. C.; Hochster, H.; Mendoza, S.; Hecht, S. S.; Crowell, J.; Chung, F. L.; *Anal. Biochem.* **2001**, *291*, 279.
14. Murase, T.; Fujita, M.; *J. Org. Chem.* **2005**, *70,* 9369.
15. Dodangeh, M.; Gharanjig, K.; Arami, M.; Atashrouz, S.; *Dyes Pigm*. **2014**, *111*, 30.
16. Tan, J. Q.; Chang, J. H.; Deng, M. Z.; *Chin. J. Chem*. **2004**, *22*, 941.
17. Chen, K. Y.; Huang, C. T.; *Int. J. Appl. Sci. Eng*. **2004**, *2*, 3.
18. Ji, Y.; Dong, C.; Kong, D.; Lu, J.; Zhou, Q.; *Chem. Eng. J.* **2015**, *263*, 45.
19. Bellini, M. I.; Pinelli, L.; dos Santos, M. E.; Scavino, A. F.; *Int. Biodeterior. Biodegrad.* **2014**, *90*, 131.
20. Srinivas, K.; Srinivas, U.; Rao, V. J.; Bhanuprakash, K; Kishore, K. H.; Murty, U. S. N.; *Bioorg. Med. Chem. Lett.* **2005**, *15*, 1121.
21. Farouk, R.; Gaffer, H. E.; *Carbohydr. Polym*. **2013**, *97*, 138.
22. Roman, G.; *Eur. J. Med. Chem*. **2015**, *89*, 743.
23. Jiang, Z.; Ma, K.; Du, J.; Li, R.; Rena, X.; Huang, T. S.; *Appl. Surf. Sci.* **2014**, *288*, 518.
24. Rizk, H. F.; Ibrahim, S. A.; El-Borai, M. A.; *Dyes Pigm.* **2015**, *112*, 86.
25. Gorensek, M.; *Dyes Pigm.* **1999**, *40,* 225.
26. Saeed, A.; Shabir, G.; *Arabian J. Chem.* **2014**, *in press*, DOI: 10.1016/j.arabjc.2014.11.010.
27. Kuplich, M. D.; Grasel, F. S.; Campo, L. F.; Rodembusch, F. S.; Stefani, V.; *J. Braz. Chem. Soc.* **2012**, *23*, 25.
28. Patel, D. R.; Patel, B. M.; Patel, N. B.; Patel, K. C.; *J. Saudi Chem. Soc*. **2014**, *18*, 245.
29. Rizk, H. F.; Ibrahim, S. A.; El-Borai, M. A.; *Dyes Pigm.* **2015**, *112*, 86.
30. Yrjölä, S.; Sarparanta, M.; Airaksinen, A. J.; Hytti, M.; Kauppinen, A.; Pasonen-Seppänen, S.; Adinolfi, B.; Nieri, P.; Manera, C.; Keinänen, O.; Poso, A.; Nevalainen, T. J.; Parkkari, T.; *Eur. J. Pharm. Sci.* **2015**, *67*, 85.
31. Lee, J. K.; Um, S. I; Kang, Y.; Baek, D. J.; *Dyes Pigm.* **2005**, *64*, 25.
32. Um, S. I.; Lee, J. K.; Kang, Y.; Baek, D. J.; *Dyes Pigm.* **2006**, *70*, 84.
33. Roohi, H.; Mohtamedifar, N.; Hejazi, F.; *Chem. Phys.* **2014**, *444*, 66.
34. Coelho, F. L.; Rodembusch, F. S.; Campo, L. F.; *Dyes Pigm.* **2014**, *110*, 134.
35. Dick, P. F.; Coelho, F. L.; Rodembusch, F. S.; Campo, L. F.; *Tetrahedron Lett*. **2014**, *55*, 3024.
36. Patil, V. S.; Padalkar, V. S.; Tathe, A. B.; Sekar, N.; *Dyes Pigm.* **2013**, *98*, 507.
37. Alves, R. M.; Rodembusch, F. S.; Habis, C.; Moreira, E. C.; *Mater. Chem. Phys*. **2014**, *148*, 833.

38. Grasel, F. S.; de Oliveira, T. E.; Netz, P. A.; *J. Braz. Chem. Soc.* **2015**, *26*, 420.
39. Holler, M. G.; Campo, L. F.; Brandelli, A.; Stefani, V.; *J. Photochem. Photobiol. A* **2002**, *149*, 217.
40. Rzeska, A.; Malicka, J.; Guzow, K.; Szabelski, M.; Wiczk, W.; *J. Photochem. Photobiol. A* **2001**, *146*, 9.
41. Matson, W. T.; *Fluorescent and Luminescent Probes for Biological Activity: a Practical Guide to Technology for Quantitative Real-time Analysis*; Academic Press: London, 1999.
42. Demmer, C. S.; Bunch, L.; *Eur. J. Med. Chem.* **2014**, *in press*, DOI: 10.1016/j.ejmech.2014.11.064.
43. Contreras, R.; Flores-Parra, A.; Mijangos, E.; Téllez, F.; López-Sandoval, H.; Barba-Behrens, N.; *Coord. Chem. Rev*. **2009**, *253*, 1979.
44. Li, H.; Guo, Y.; Lei, Y.; Gao, W.; Liu, M.; Chen, J.; Hu, Y.; Huang, X.; Wu, H.; *Dyes Pigm.* **2015**, *112*, 105.
45. Song, B.; Zhuang, Q.; Ying, L.; Liu, X.; Han, Z.; *Polym. Degrad. Stab.* **2012**, *97*, 1569.
46. Kim, S. H.; Park, S.; Kwon, J. E.; Park, S. Y.; *Adv. Funct. Mater*. **2011**, *21*, 644.
47. Shono, H.; Ohkawa, T.; Tomoda, H.; Mutai, T.; Araki, K.; *ACS Appl. Mater. Interfaces* **2011**, *3*, 654.
48. Liang, Z.; Liu, Z.; Jiang, L.; Gao, Y.; *Tetrahedron Lett.* **2007**, *48*, 1629.
49. Hoffmann, H. S.; Stefani, V.; Benvenutti, E. V.; Costa, T. M. H.; Gallas, M. R.; *Mater. Chem. Phys.* **2011**, *126*, 97.
50. Campo, L. F.; Corrêa, D. S.; Araújo, M. A.; Stefani, V.; *Macromol. Rapid Commun*. **2000**, *21*, 832.
51. Woolfe, G. J.; Melzig, M.; Schneider, S.; Dorr, F.; *Chem. Phys*. **1983**, *77*, 127.
52. Verdasco, G.; Martín, M. A.; del Castillo, B.; López-Alvarado, P.; Menéndez, P. C.; *Anal. Chim. Acta* **1995**, *303*, 73.
53. Santra, S.; Krishnamoorthy, G.; Dogra, S. K.; *Chem. Phys. Lett.* **1999**, *311*, 55.
54. Krishnamoorthy, G.; Dogra, S. K.; *J. Lumin.* **2000**, *92*, 103.
55. Krishnamoorthy, G.; Dogra, S. K.; *J. Lumin.* **2000**, *92*, 91.
56. Rodembusch, F. S.; Campo, L. F.; Leusin, F. P.; Stefani, V.; *J. Lumin.* **2007**, *126*, 728.

Submitted: March 18, 2015
Published online: June 9, 2015

FAPERGS/CAPES has sponsored the publication of this article.

J. Braz. Chem. Soc., Vol. 26, No. 12, S1-S14, 2015.
Printed in Brazil - ©2015 Sociedade Brasileira de Química
0103 - 5053 $6.00+0.00

Supplementary Information

Synthesis and Photophysical Characterization of Novel ESIPT Triazinyl-Benzazole Derivatives

Fábio S. Grasel,*[,a,b] Fabiano Barreto,[c] Louise Jank[a,c] and Valter Stefani*[,a]

[a]*Instituto de Química, Universidade Federal do Rio Grande do Sul, CP 15003, 91501-970 Porto Alegre-RS, Brazil*

[b]*Programa de Pós-graduação em Engenharia e Tecnologia de Materiais, Pontifícia Universidade Católica do Rio Grande do Sul, CP 1429, 90619-900 Porto Alegre-RS, Brazil*

[c]*Laboratório Nacional Agropecuário - LANAGRO/RS, Ministério da Agricultura, Pecuária e Abastecimento, 91780-580 Porto Alegre-RS, Brazil*

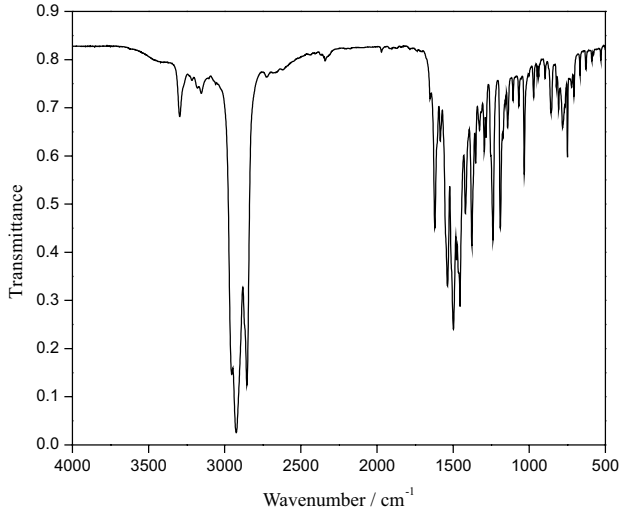

Figure S1. IR spectrum (nujol) of compound **3a**.

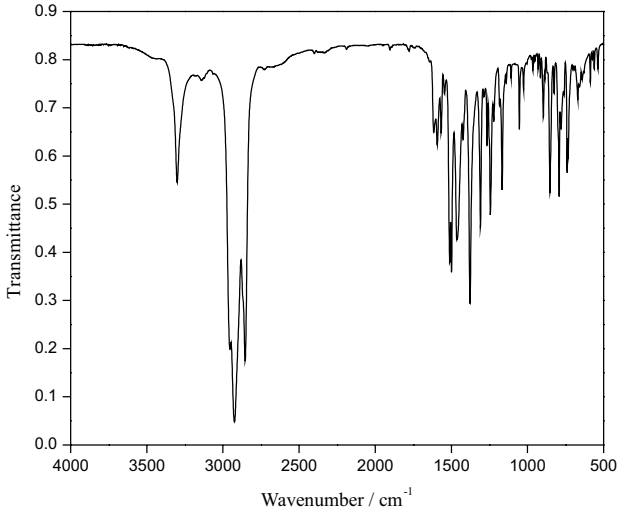

Figure S2. IR spectrum (nujol) of compound **3b**.

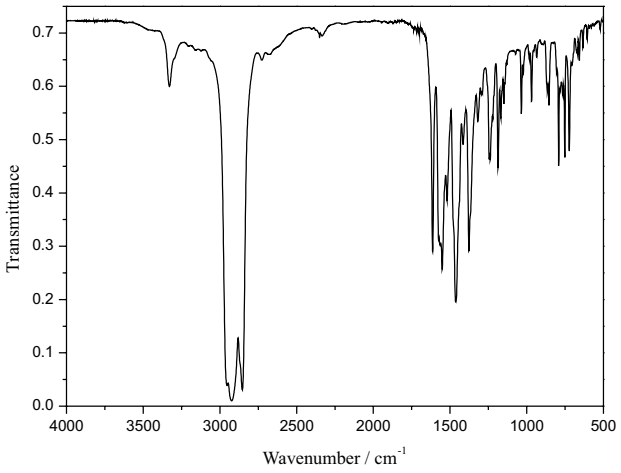

Figure S3. IR spectrum (nujol) of compound **3c**.

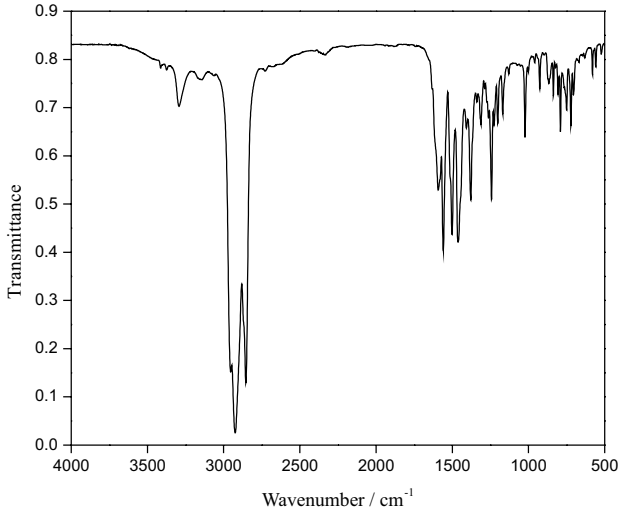

Figure S4. IR spectrum (nujol) of compound **3d**.

*e-mail: fsgrasel@gmail.com, vstefani@iq.ufrgs.br

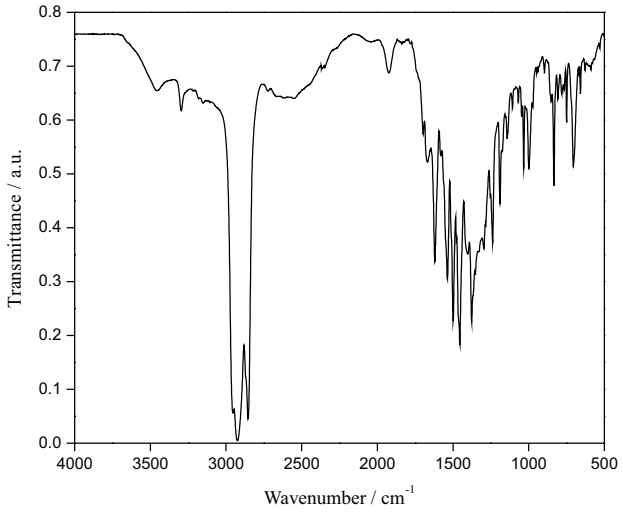

Figure S5. IR spectrum (nujol) of compound **4a**.

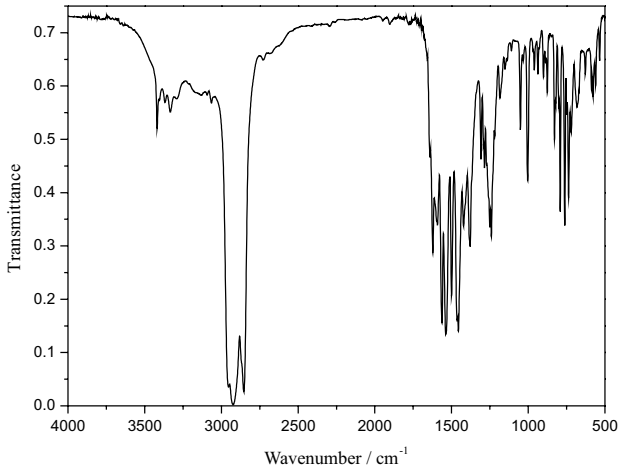

Figure S6. IR spectrum (nujol) of compound **4b**.

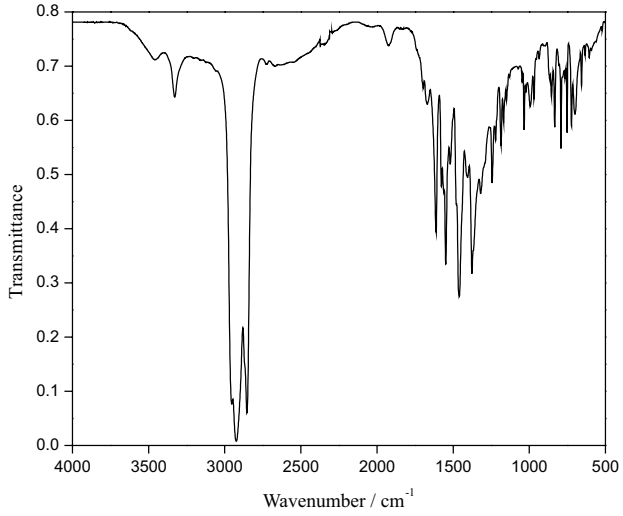

Figure S7. IR spectrum (nujol) of compound **4c**.

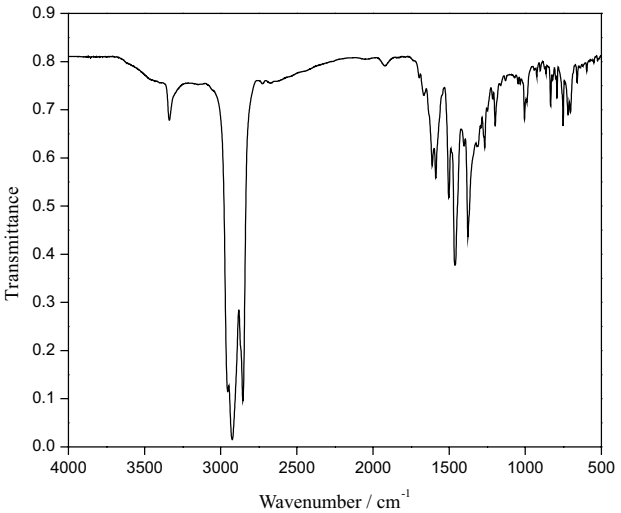

Figure S8. IR spectrum (nujol) of compound **4d**.

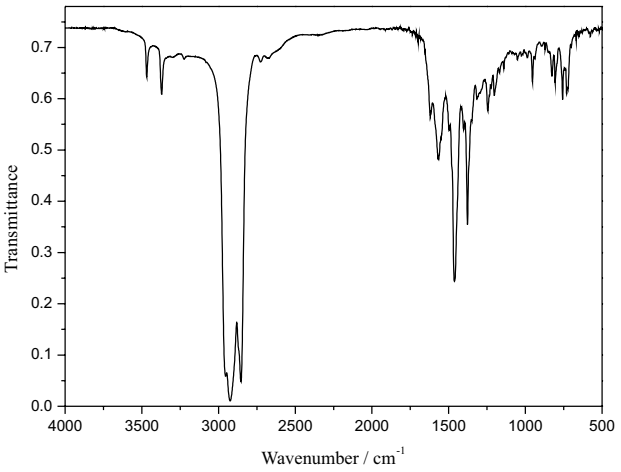

Figure S9. IR spectrum (nujol) of compound **5a**.

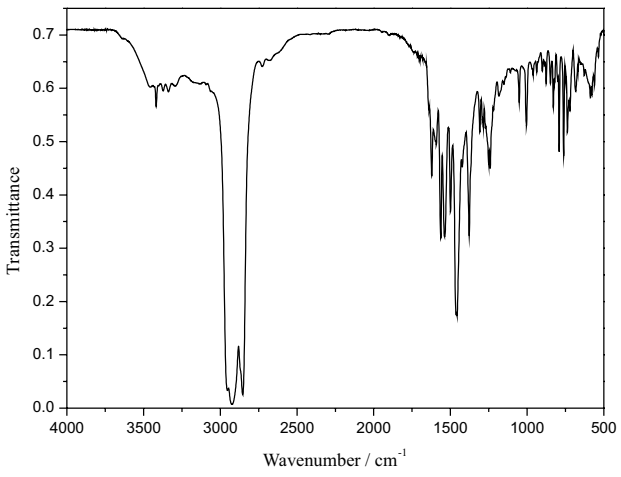

Figure S10. IR spectrum (nujol) of compound **5b**.

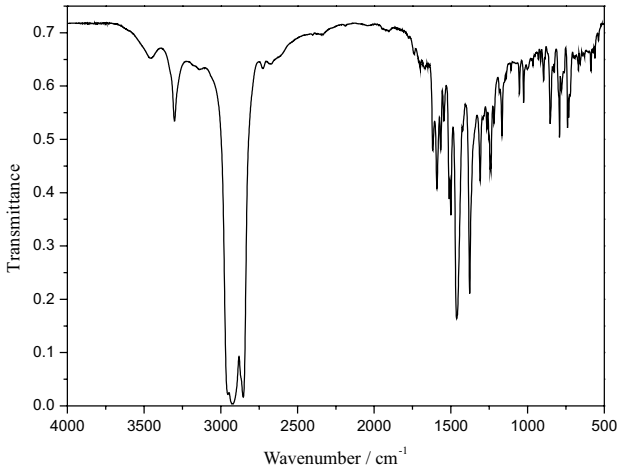

Figure S11. IR spectrum (nujol) of compound **5c**.

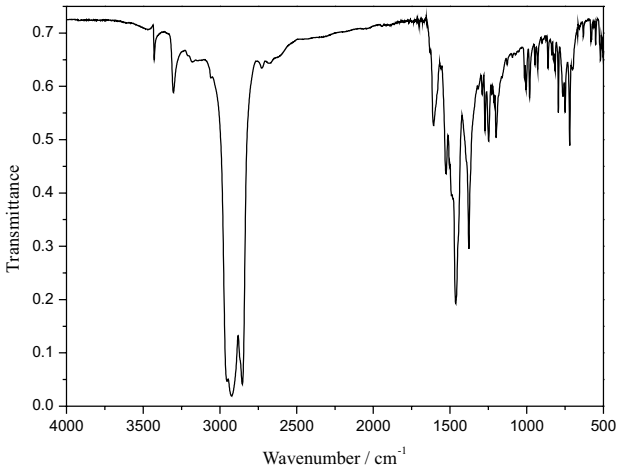

Figure S12. IR spectrum (nujol) of compound **5d**.

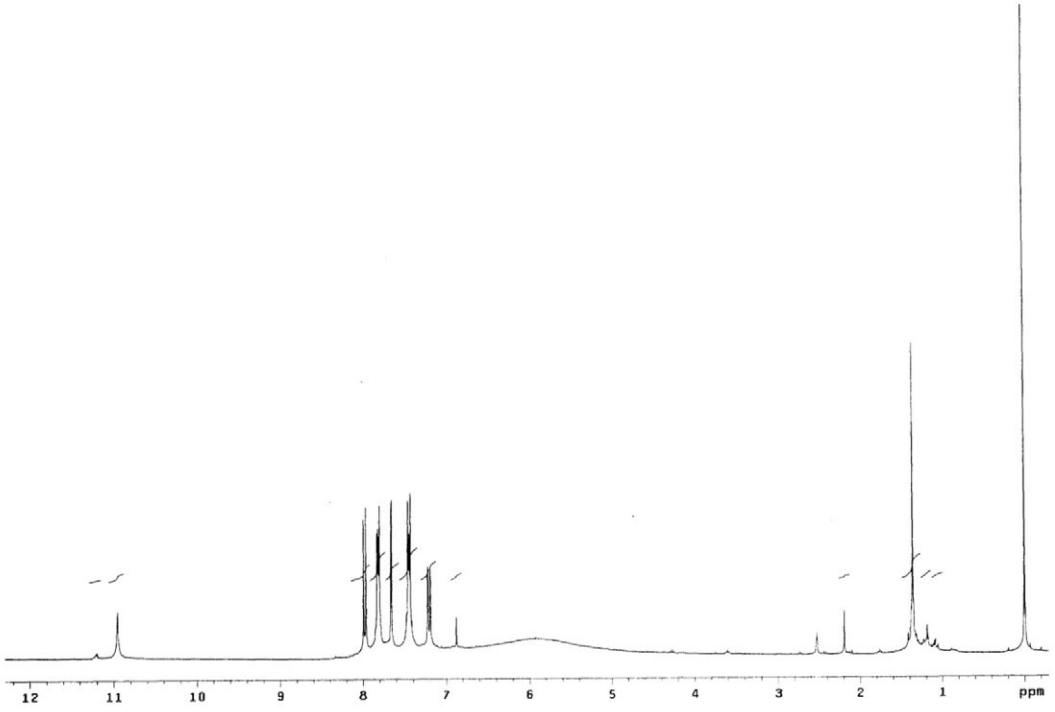

Figure S13. ^{1}H NMR spectrum (300 MHz, DMSO-d_6) of compound **3a**.

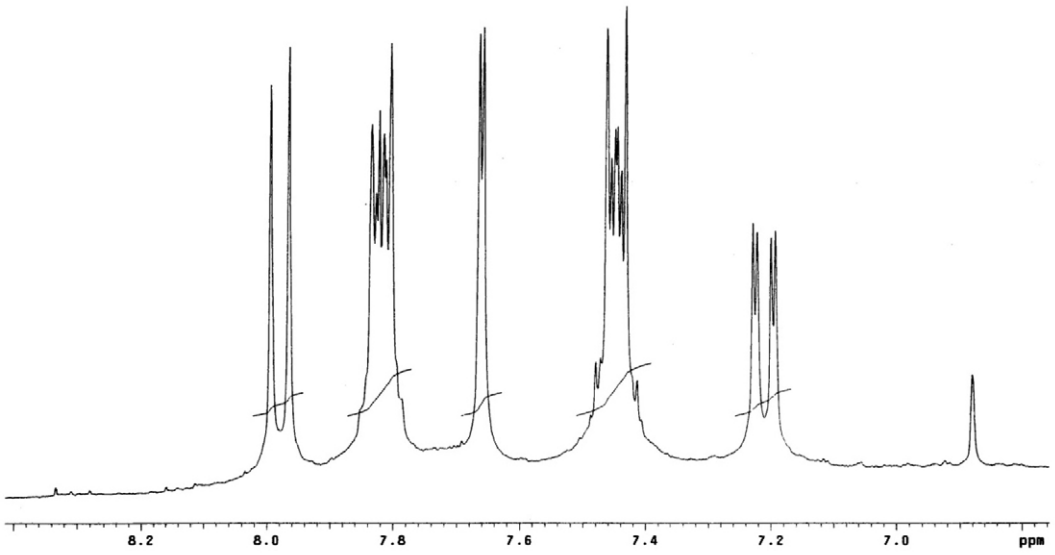

Figure S14. ^{1}H NMR spectrum (300 MHz, DMSO-d_6) of compound **3a**.

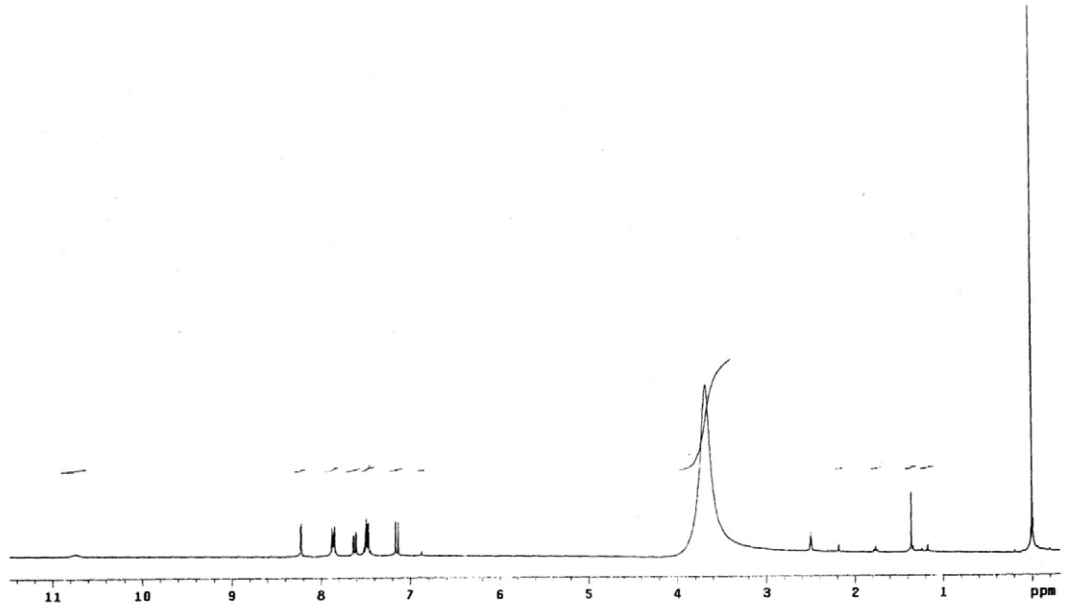

Figure S15. ^{1}H NMR spectrum (300 MHz, DMSO-d_6) of compound **3b**.

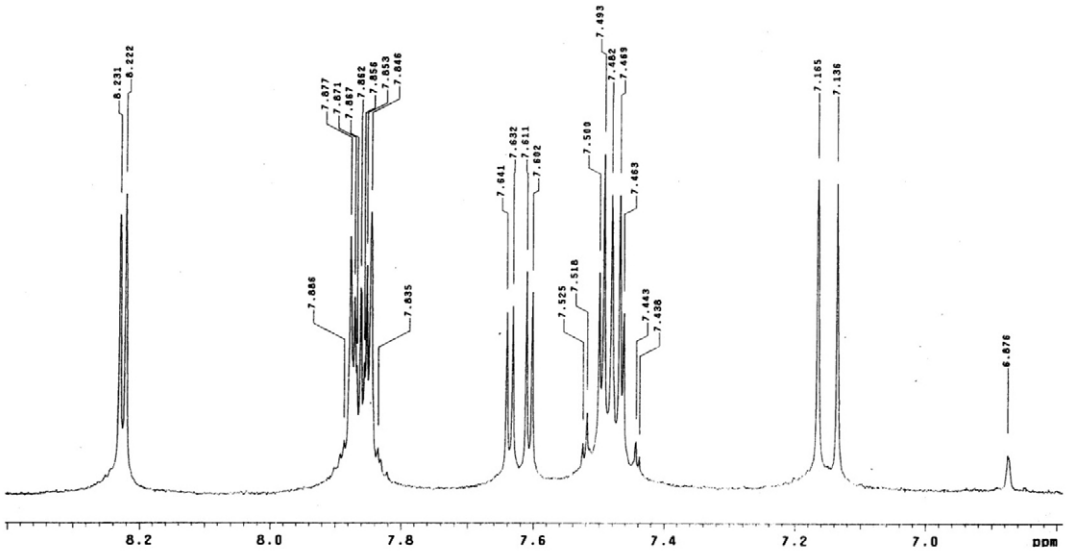

Figure S16. ^{1}H NMR spectrum (300 MHz, DMSO-d_6) of compound **3b**.

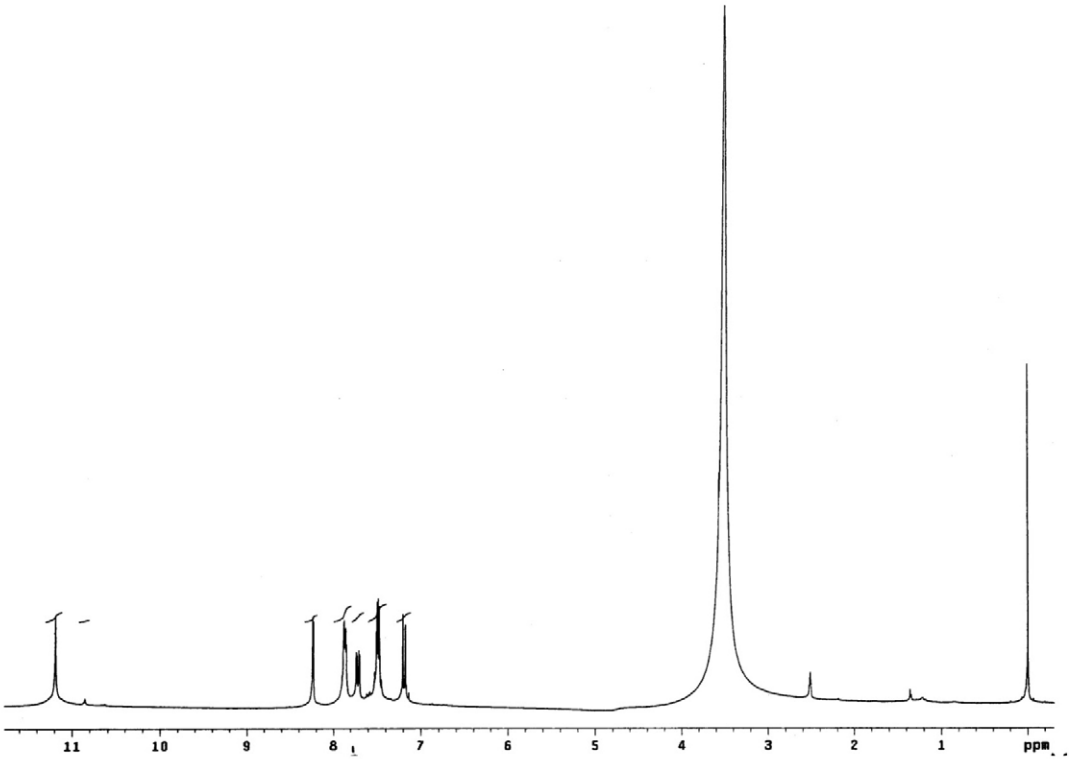

Figure S17. ^{1}H NMR spectrum (300 MHz, DMSO-d_6) of compound **3c**.

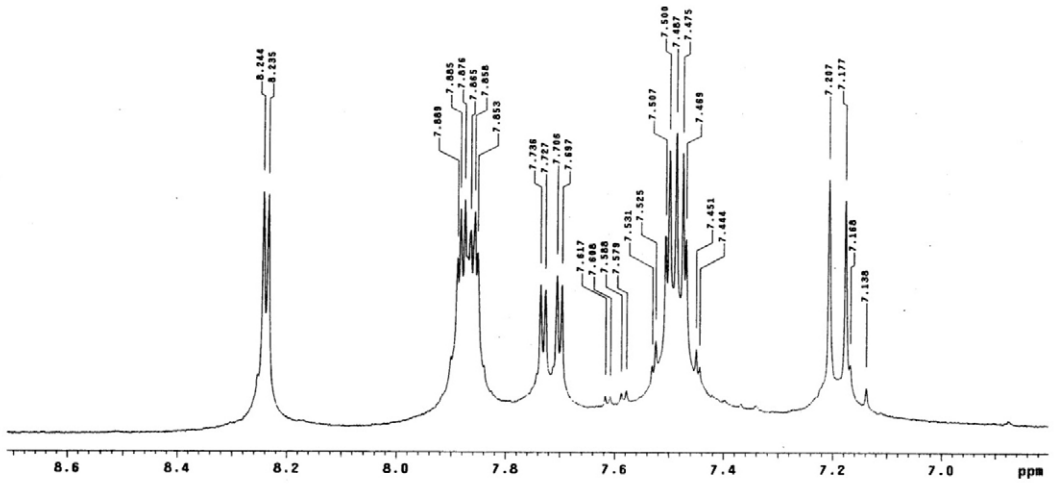

Figure S18. ^{1}H NMR spectrum (300 MHz, DMSO-d_6) of compound **3c**.

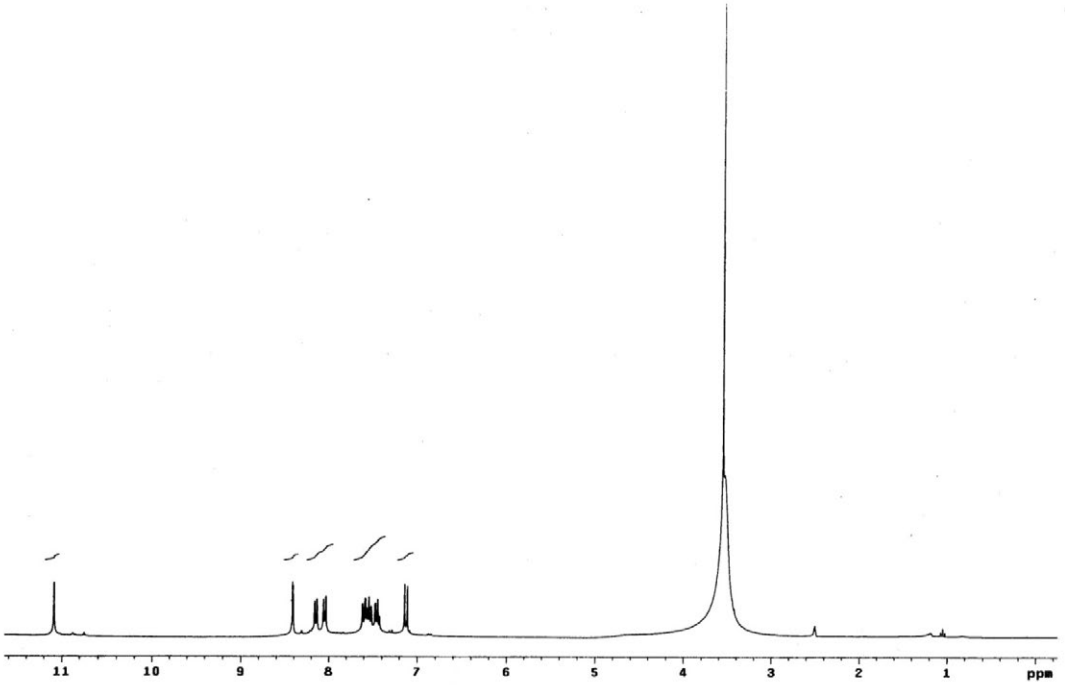

Figure S19. ^{1}H NMR spectrum (300 MHz, DMSO-d_6) of compound **3d**.

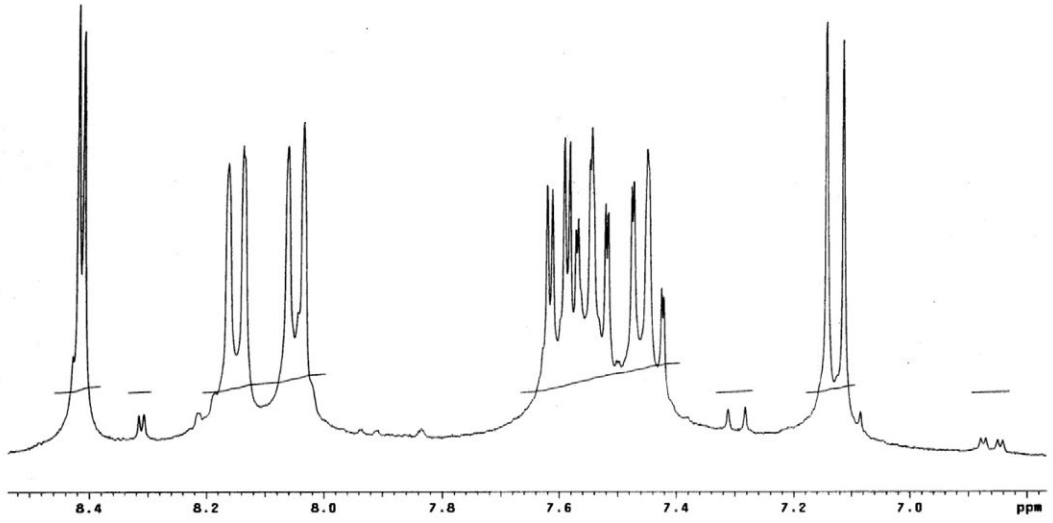

Figure S20. ^{1}H NMR spectrum (300 MHz, DMSO-d_6) of compound **3d**.

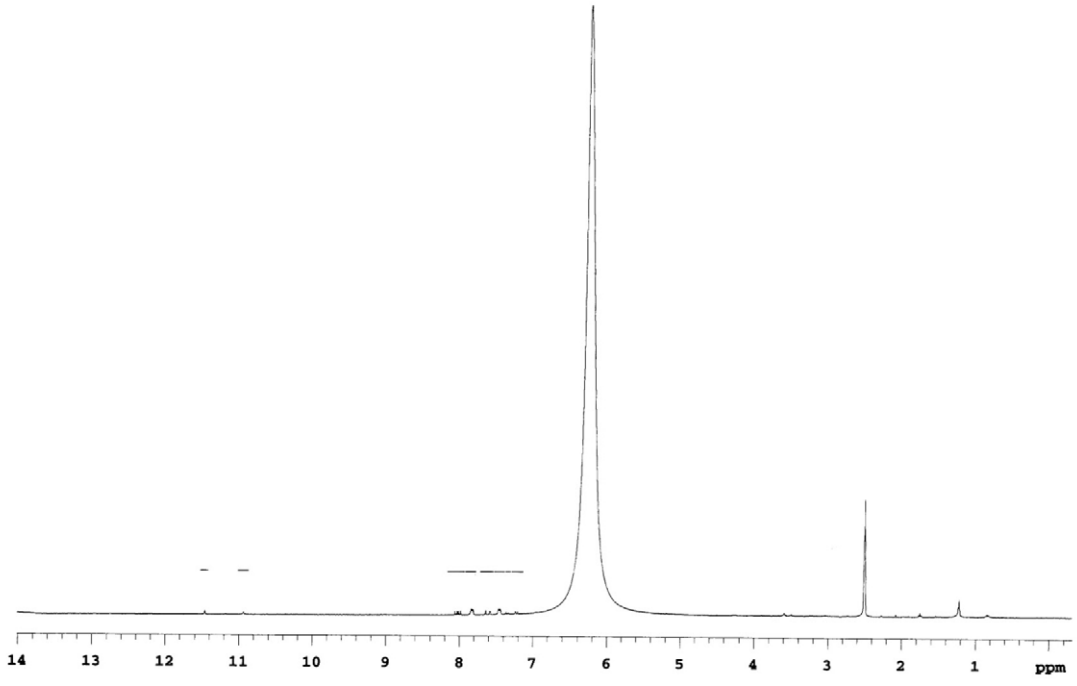

Figure S21. ^{1}H NMR spectrum (300 MHz, DMSO-d_6) of compound **4a**.

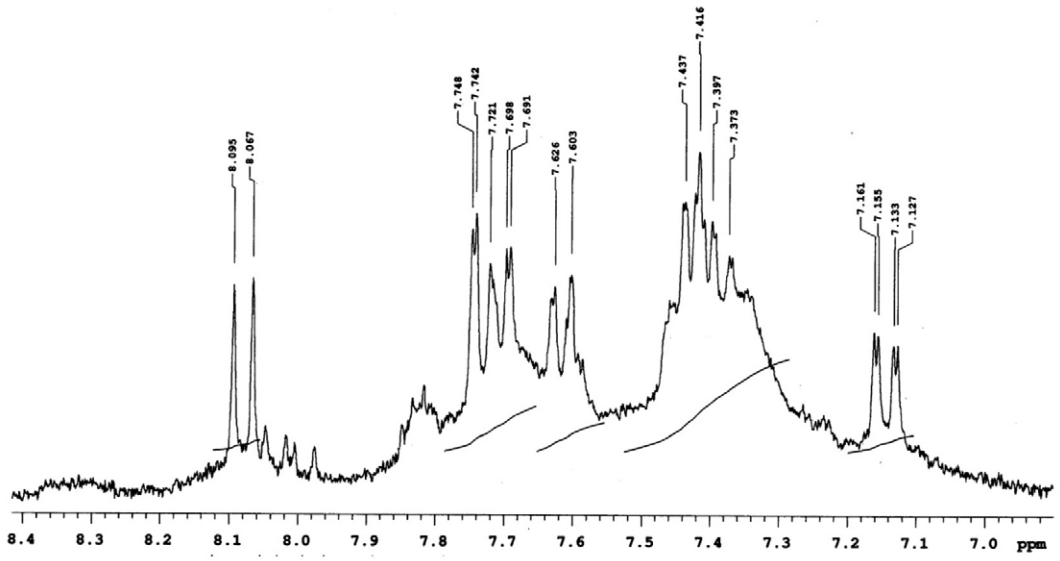

Figure S22. ^{1}H NMR spectrum (300 MHz, DMSO-d_6) of compound **4a**.

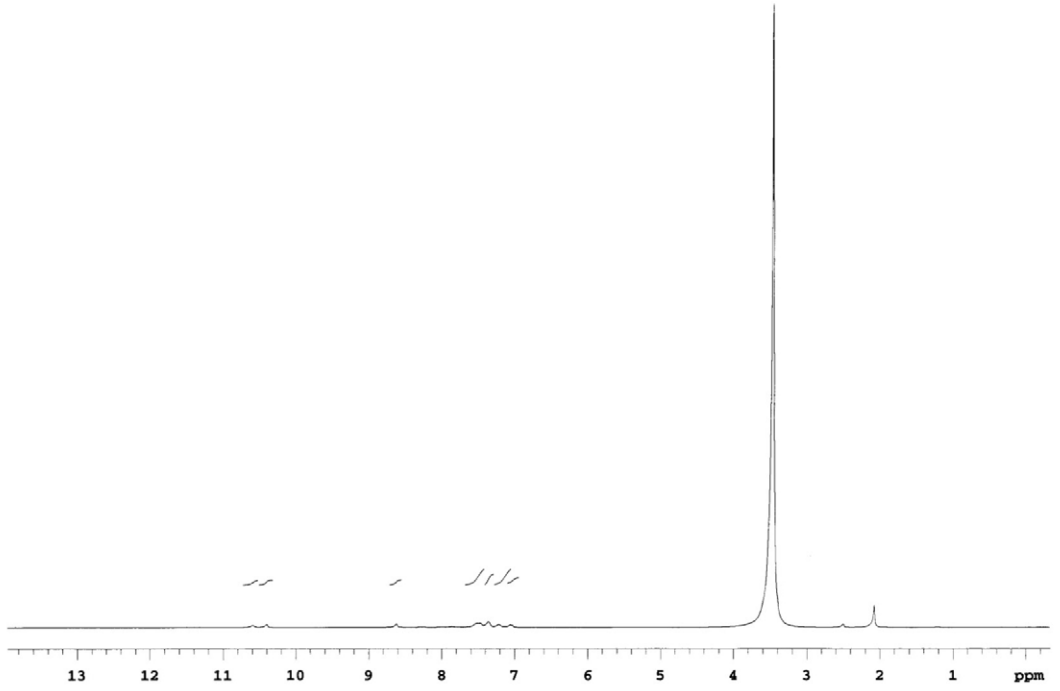

Figure S23. ^{1}H NMR spectrum (300 MHz, DMSO-d_6) of compound **4b**.

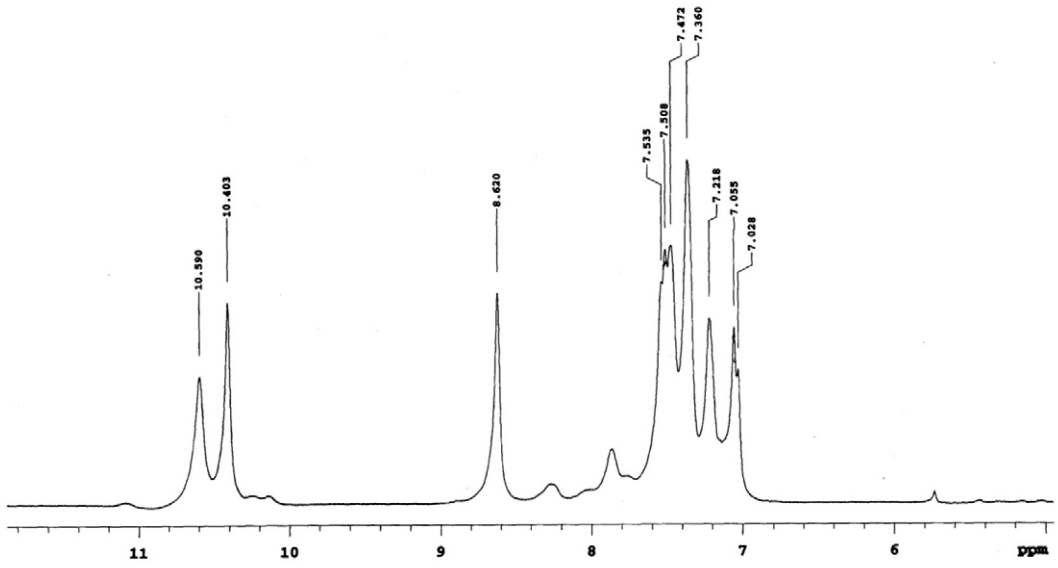

Figure S24. ^{1}H NMR spectrum (300 MHz, DMSO-d_6) of compound **4b**.

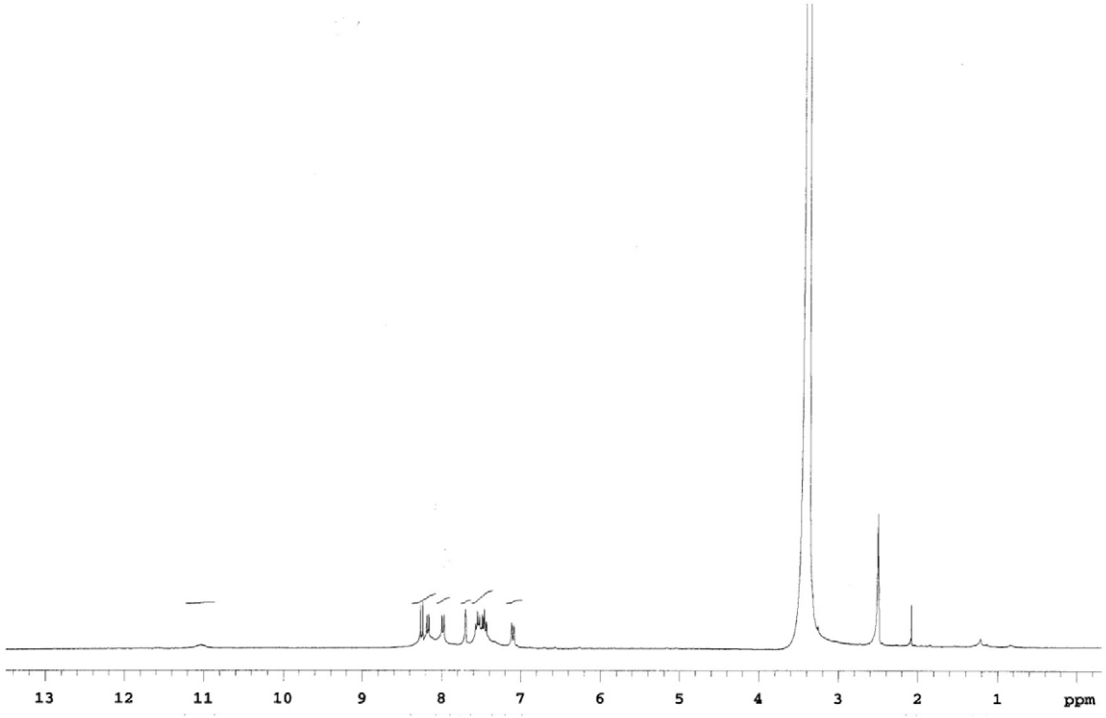

Figure S25. ^{1}H NMR spectrum (300 MHz, DMSO-d_6) of compound **4c**.

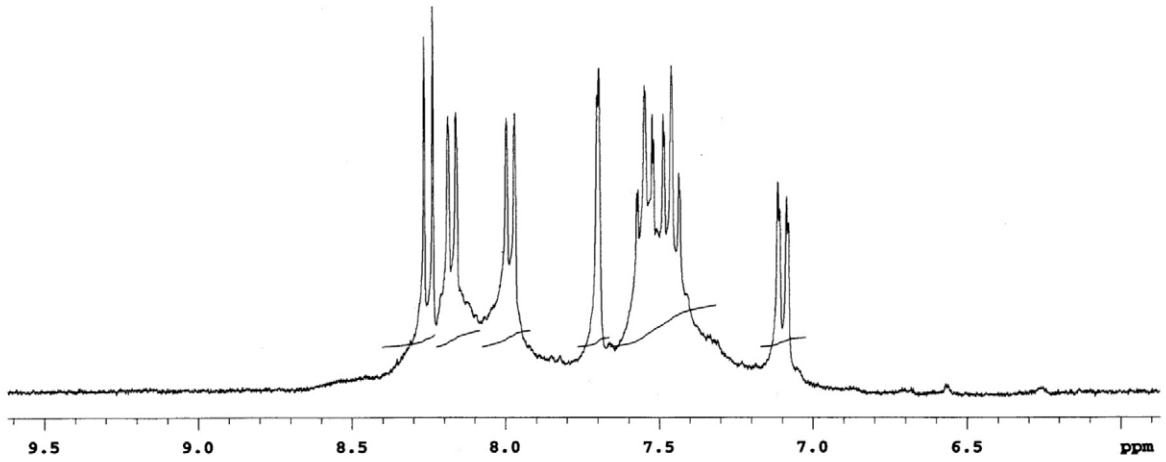

Figure S26. ^{1}H NMR spectrum (300 MHz, DMSO-d_6) of compound **4c**.

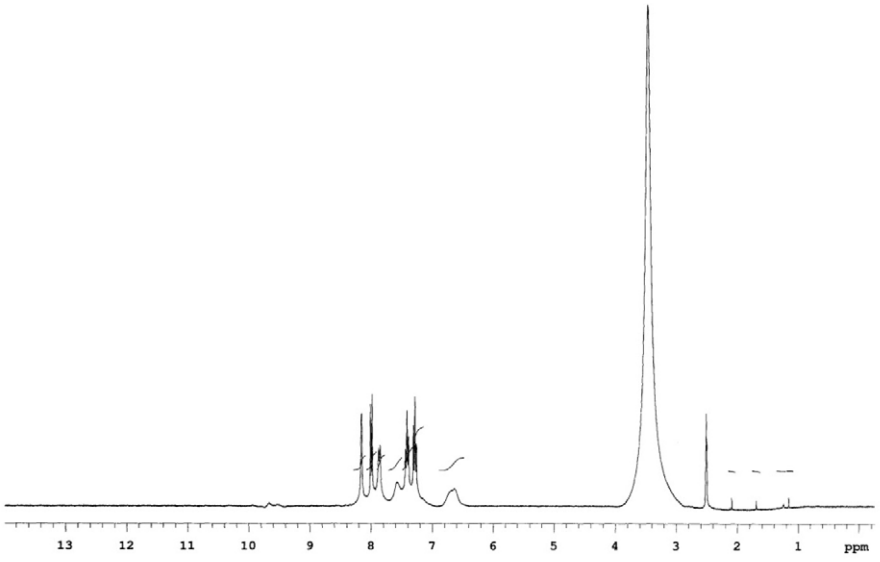

Figure S27. ^{1}H NMR spectrum (300 MHz, DMSO-d_6) of compound **4d**.

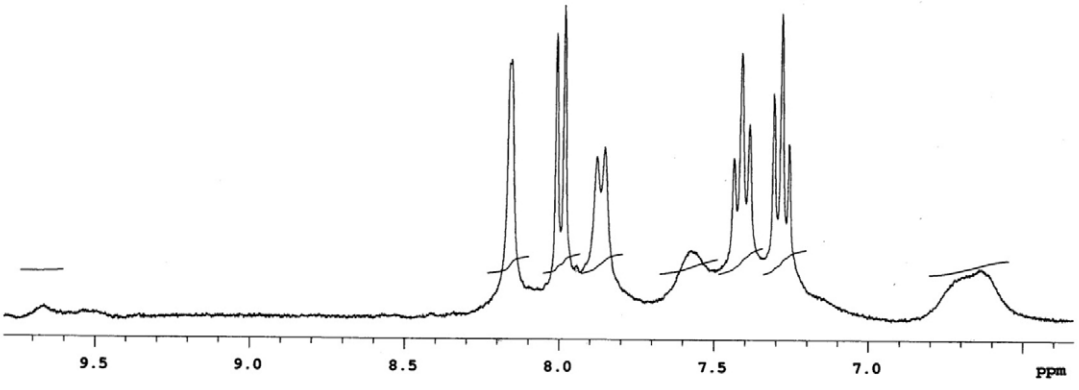

Figure S28. ^{1}H NMR spectrum (300 MHz, DMSO-d_6) of compound **4d**.

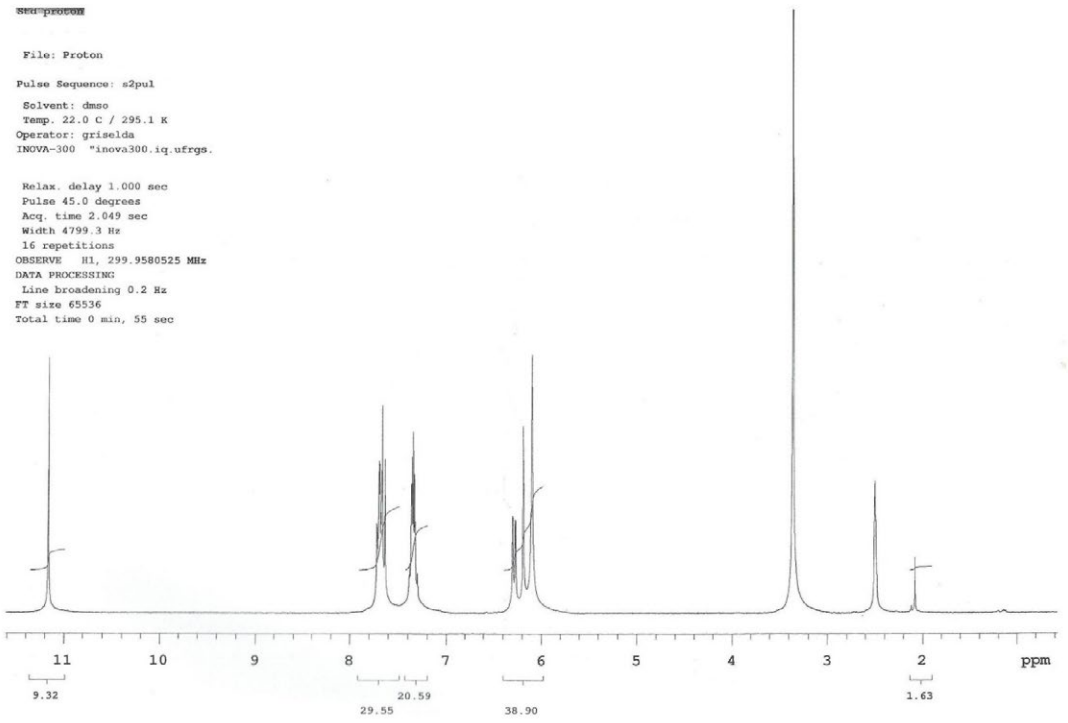

Figure S29. ^{1}H NMR spectrum (300 MHz, DMSO-d_6) of compound **5a**.

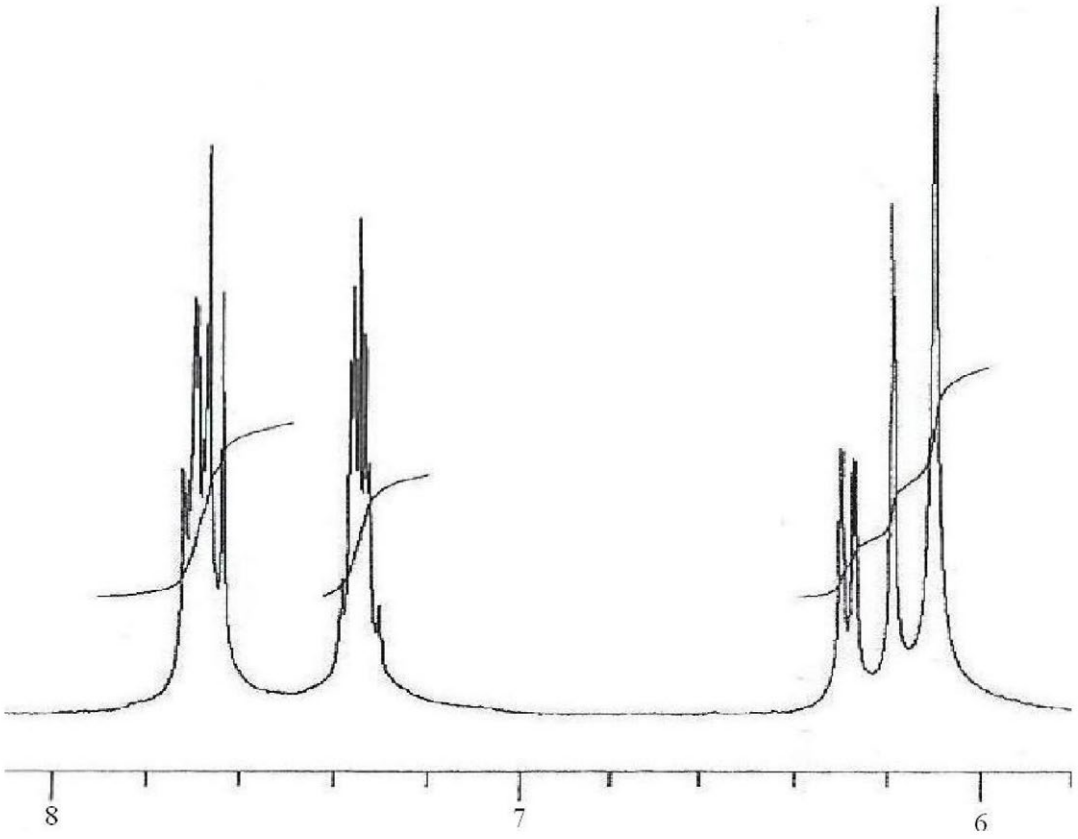

Figure S30. ^{1}H NMR spectrum (300 MHz, DMSO-d_6) of compound **5a**.

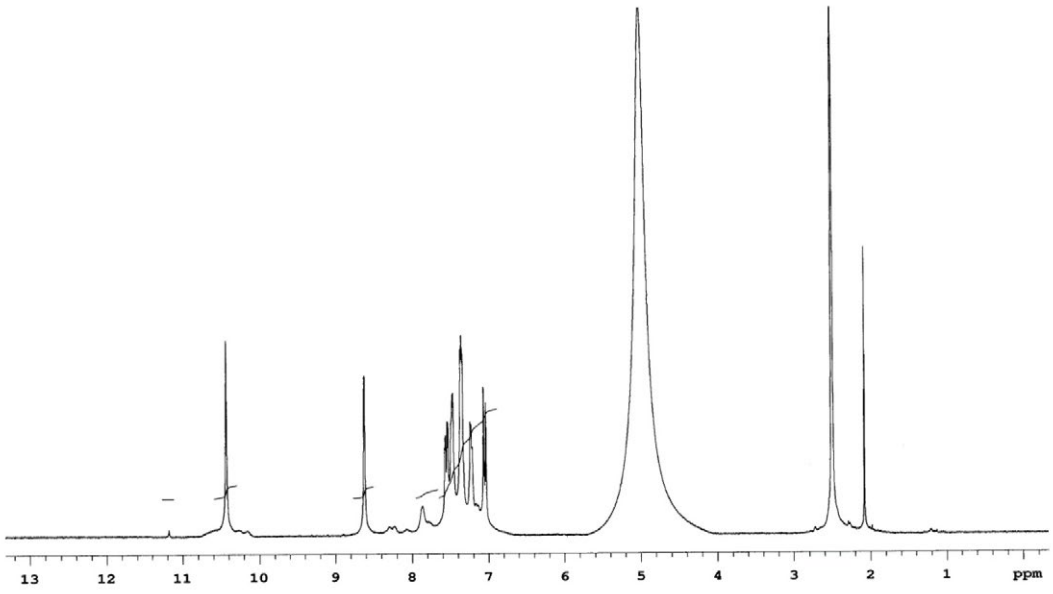

Figure S31. ^{1}H NMR spectrum (300 MHz, DMSO-d_6) of compound **5b**.

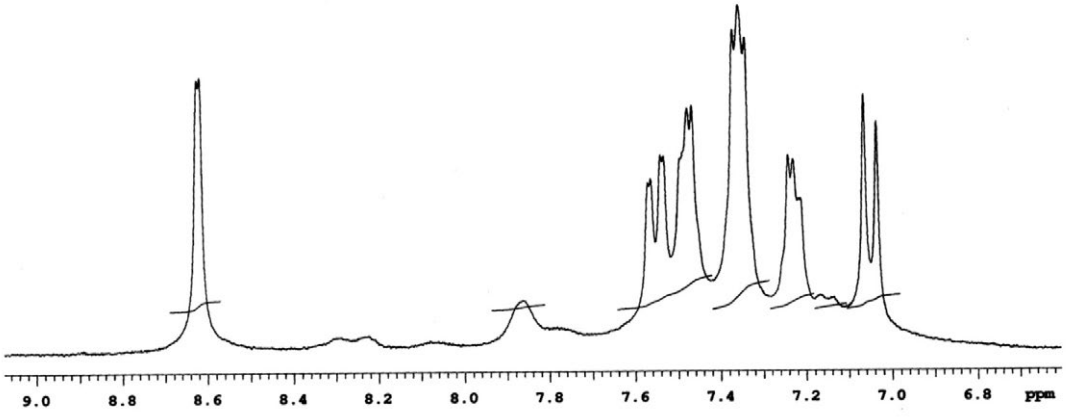

Figure S32. ^{1}H NMR spectrum (300 MHz, DMSO-d_6) of compound **5b**.

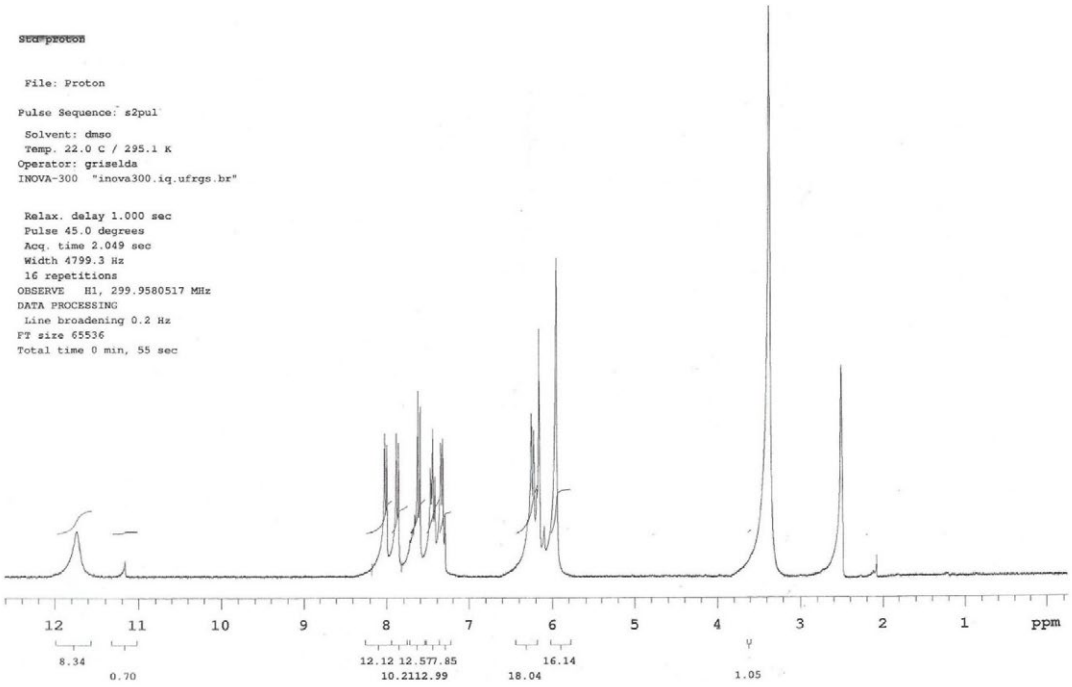

Figure S33. ^{1}H NMR spectrum (300 MHz, DMSO-d_6) of compound **5c**.

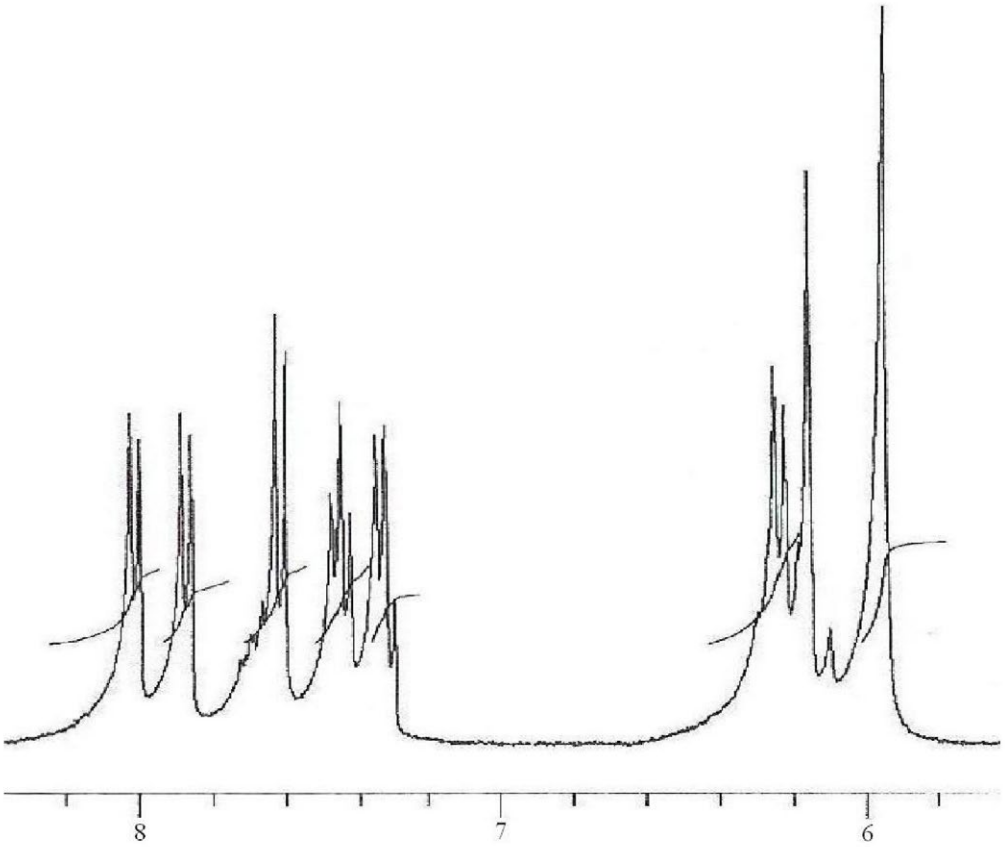

Figure S34. ^{1}H NMR spectrum (300 MHz, DMSO-d_6) of compound **5c**.

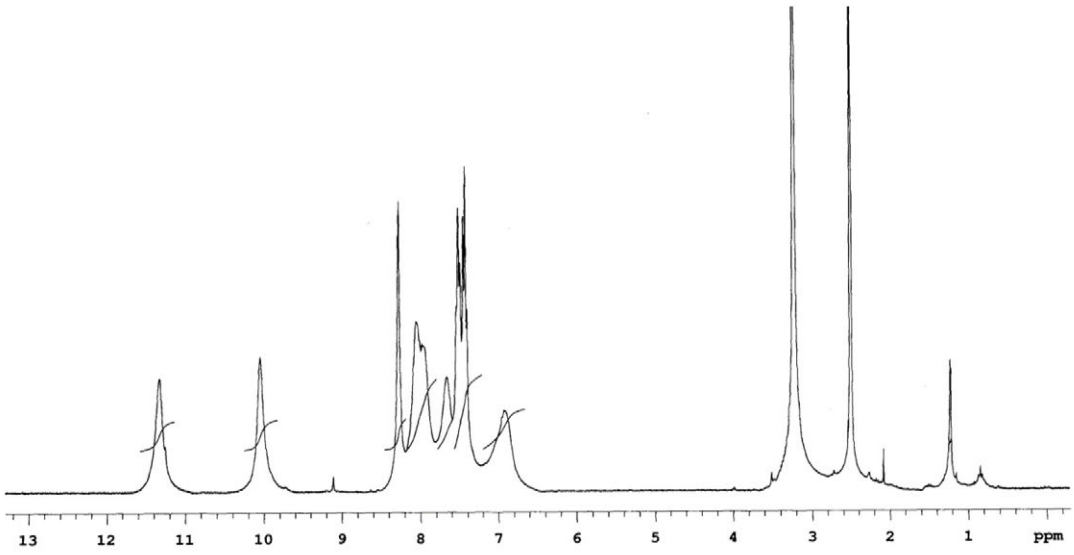

Figure S35. ^{1}H NMR spectrum (300 MHz, DMSO-d_6) of compound **5d**.

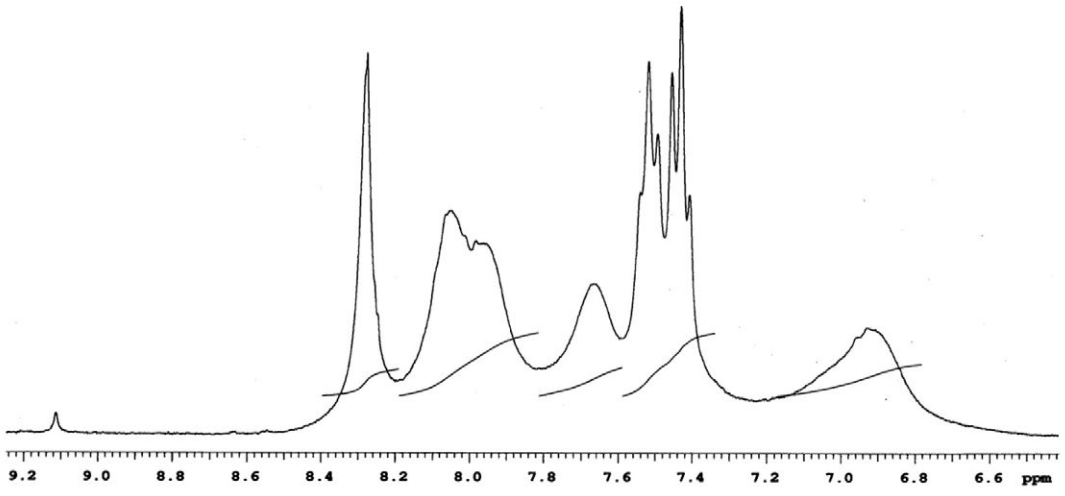

Figure S36. ^{1}H NMR spectrum (300 MHz, DMSO-d_6) of compound **5d**.